Analysis of the Spectra of Jahn-Teller Distorted Radicals

UNDERGRADUATE RESEARCH THESIS

Presented in Partial Fulfillment of the Requirements for graduation "with Honors Research Distinction in Chemistry" in the College of Arts and Sciences of The Ohio State University

By

Scott M. Garner,

Undergraduate Program in Chemistry

The Ohio State University

2018

Thesis Committee:

Professor Terry A. Miller, Department of Chemistry and Biochemistry, Advisor

Professor Robert Baker, Department of Chemistry and Biochemistry

Professor Chris Otter, Department of History

Abstract

Defining appropriate potential energy surfaces (PES) for Jahn-Teller active molecules remains problematic due to the breakdown of the Born-Oppenheimer approximation. Quantification of the magnitude of the Jahn-Teller geometric distortions is required for regaining understandings of molecular and spectroscopic properties of these molecules. Recent experimental spectra of the cyclopentadienyl radical, C_5H_5, challenge theoretical understandings of the Jahn-Teller effect. Generalized methodology is developed utilizing *ab-initio* electronic structure calculations in concert with vibronic eigenfunctions in order to determine the Watson term, h_1, an element of rotational model. Tabulated h_1 values provide insights to rotational structure of vibrational bands for experimental identification as well as further understanding of the Jahn-Teller potential surfaces. Features of the cyclopentadienyl radical spectra are predicted using this method. Application to the nitrate radical, NO_3, underscores insufficiencies in parameterized potentials used in the case of strong Jahn-Teller coupling.

Acknowledgments

First and foremost, I need to thank Dr. Miller for guiding and supporting me through not only my undergraduate research experience but also the process transforming from an undergraduate to a future scientist. I also need to thank Dr. McCoy for plucking me out of my honors general chemistry class to begin research. Even though she left me, she has been a mentor to me ever since, and I am ever grateful for her continued support.

So far as the Miller group is concerned, I'd like to thank Dr. Ketan Sharma for always keeping me honest, Dr. Meng Huang for being a good friend even though he left too, Henry Tran for his guidance and leaving all of his undergraduate work on the pub drive so I had material to look at, and Yi Yan for reminding me how exciting it is to be involved in research as an undergrad. I'd also like to thank the Barry Goldwater and Astronaut Scholarship Foundations for believing in me and supporting my work, as well as the Chemistry and Biochemistry Department for all that they have provided for me.

A huge thanks goes out to all of my undergrad professors, advisors, mentors, and friends for all I've learned from them and the encouragement to be my best self. Finally, of course I have to thanks my parents, Eileen and Randy Garner, for their endless love and support, no matter how many frantic texts they received at 4 in the morning. Without their support I could not have made it this far.

Table of Contents

Chapter 1
Introduction

1.1 Radical Chemistry

Without a complete understanding of fundamental reactions and molecular processes, efforts to designs complex synthesis and optimize chemical processes we depend upon would be futile. From hydrocarbon combustion, a reaction that has been utilized by humans for thousands of years to oxidation and photolysis of atmospheric gases, even reactions that involve only a handful of atoms are highly complex processes. A common theme in studying these reactions involves understanding the roles of intermediate radical species. Radicals, by definition, have unpaired electrons, causing these molecules to be highly reactive and play important roles in reaction mechanisms. Understanding how and why these radical molecules influence the products of chemical reactions is vital not only for understanding the world around us, but controlling the chemistry of a world increasingly influenced by human activity.

1.2 Spectroscopic Tools

A fundamental issue for chemistry is the inability to directly observe molecules during reactions. Spectroscopic methods are vital probes, which provide insight into not only the presence and concentration of reactive intermediates, but also provide crucial information about the structure and reactivity of these molecules. Modern spectroscopic methods can study not just immense numbers of molecules, but numerous physical properties of each

molecules. However, in complex mixtures like hydrocarbon combustion, when a wide array of similar molecules are all present for short times, the spectra become incredibly complex. Modern theoretical methods provide useful information for understanding these convoluted spectra and are well suited for assigning spectral features to specific molecules and molecular phenomena. However, both spectroscopic and theoretical methods have shortcomings–the focus of this thesis, understanding the Jahn-Teller effect, is one such example.

1.3 Molecules

Two well known radical molecules that display Jahn Teller effects are the nitrate radical, NO_3, and the cyclopentadienyl radical, C_5H_5. The first spectra of the nitrate radical was likely taken in 1882, before the quantum theory needed to understand these results began to percolate through leading communities of physicists.[1] The first systematic investigation of this reactive intermediate is attributed to Jones and Wulf in 1937.[2] NO_3 is known to be the primary oxidant in the night sky.[3] Recent studies have shown that up to 33% of natural organic nitrates are produced through nitrate radical chemistry.[4] C_5H_5 plays an important role in fuel combustion, and has been spectroscopically studied for over half a century.[5] The first theoretical study of C_5H_5 was completed in 1960.[6] These two molecules are both intermediate radical species with rich histories, yet many aspects of both remain ambiguous to scientists to this day.

Chapter 2
Methodology

The Jahn-Teller effect is a well known molecular phenomena where electronic degeneracies are broken via geometric distortions gaining a net energetic stabilization. Asymmetric distortions from the equilibrium geometry creates conical intersections on electronic potential energy surfaces, leading to the break down of the Born-Oppenheimer approximation. Quantification of the magnitude of the Jahn-Teller effect can be done via fitting experimental spectra, however a theoretical method toward quantification has remained unavailable. In this chapter, the quantum mechanical basis of the Jahn-Teller effect is presented followed by the derivation of methodology that will be used to predict the 'Watson Term', h_1, an element of the Jahn-Teller rotational Hamiltonian.

2.1 Hamiltonian

Quantum mechanically, we can completely describe system by its wavefunction, denoted Ψ. All possible information regarding the system, which from this point forward will be considered to be a molecule, is determined by this wavefunction. Gaining access to any observable quantity is done through the application of linear operators. One primary goal of quantum mechanics is the solution of the time independent Schrödinger equation,

$$\hat{\mathcal{H}}\Psi = E\Psi \tag{2.1}$$

where $\hat{\mathcal{H}}$ is the Hamiltonian E is the total energy of the system.

The Hamiltonian can be expanded as

$$\hat{\mathcal{H}} = \hat{T}_e + \hat{T}_N + \hat{V}_{ee} + \hat{V}_{eN} + \hat{V}_{NN} \tag{2.2}$$

$$\hat{T}_e = -\sum_i \frac{\hbar^2}{2m_e}\nabla_i^2 \tag{2.3a}$$

$$\hat{T}_N = -\sum_k \frac{\hbar^2}{2M_k}\nabla_k^2 \tag{2.3b}$$

$$\hat{V}_{ee} = \sum_i \sum_{j>i} \frac{e^2}{4\pi\epsilon_0|\mathbf{r}_i - \mathbf{r}_j|} \tag{2.3c}$$

$$\hat{V}_{eN} = \sum_i \sum_{k>i} \frac{Z_k e^2}{4\pi\epsilon_0|\mathbf{r}_i - \mathbf{R}_k|} \tag{2.3d}$$

$$\hat{V}_{NN} = \sum_k \sum_{l>k} \frac{Z_k Z_l e^2}{4\pi\epsilon_0|\mathbf{R}_k - \mathbf{R}_l|} \tag{2.3e}$$

where $\hat{T}$ are kinetic energy terms, $\hat{V}$ are potential energy terms, indexes i, j refer to individual electrons, while indexes k, l specify nuclei. The $\mathbf{r_i}$ refers to the position of the i^{th} electron with mass m_e and $\mathbf{R_k}$ refers to the position of the k^{th} nuclei with mass M_k and charge $Z_k e$ where Z_k is the number of protons. $\hbar$ and ϵ_0 are reduced Planck's constant and the permittivity of free space, respectively, and e is the electron fundamental charge. Denoting the total ensemble of nuclear coordinates as $\mathbf{R} = (\mathbf{R}_1, ..., \mathbf{R}_N)$ and electron coordinates as $\mathbf{r} = (\mathbf{r}_1, ..., \mathbf{r}_n)$, the Schrödinger equation is expressed as

$$\hat{\mathcal{H}}\Psi(\mathbf{r}, \mathbf{R}) = E_{tot}(\mathbf{r}, \mathbf{R})\Psi(\mathbf{r}, \mathbf{R}) \tag{2.4}$$

Solving for the eigenfunctions and eigenvalues, or total energies, of Equation 2.4 is central to molecular quantum mechanics and spectroscopy.

2.1.1 The Born-Oppenheimer Approximation

For systems as simple as helium, Equation 2.4 has no analytic solution, meaning for most systems approximations are required to achieve approximate solutions. An almost universal approach is to utilize the Born-Oppenheimer approximation which assumes stationary nuclei. This approximation is rationalized in that electrons are significantly lighter than nuclei ($m_e << m_p$), and during the time scale of electronic motion, the nuclei remain essentially stationary.[7] The coordinates and interactions of electrons are then parameterized based on the nuclear coordinates such that

$$\hat{\mathcal{H}}_e \Psi(\mathbf{r}; \mathbf{R}) = E_e \Psi(\mathbf{r}; \mathbf{R}) \tag{2.5}$$

where now the E_e is the electronic energy solved at a specific nuclear geometry, $\mathbf{R}$. In this approximation the total Hamiltonian of Equation 2.2 can be split into an electronic component, $\hat{\mathcal{H}}_e$, and a nuclear component $\hat{\mathcal{H}}_N$

$$\hat{\mathcal{H}}_e = \hat{T}_e + \hat{V}_{ee} + \hat{V}_{eN} \tag{2.6}$$

$$\hat{\mathcal{H}}_N = \hat{T}_N + \hat{V}_{NN} \tag{2.7}$$

while the total wavefunction can be expressed as

$$\Psi(\mathbf{r} : \mathbf{r}) = \Psi_e \Psi_N \tag{2.8}$$

where Ψ_e is an electronic component that is an eigenfunction of the electronic Hamiltonian and likewise Ψ_N is an eigenfunction of the nuclear Hamiltonian. In these ways, approximate solutions to the time independent Schrödinger equation are accessible.

2.2 The Jahn-Teller Problem

The Jahn-Teller theorem states that in a molecule in an electronically degenerate state under proper symmetry bound conditions will distort its geometry and lower its symmetry.[8] The lifting of the electronic degeneracy correspondingly leads to a lower total energy. How the molecule distorts is dependent upon the symmetry of the electronic state and the symmetries

of the normal vibrational modes. For the cyclopentadienyl radical the degenerate $\widetilde{X}^2E_1''$ ground state allows for linear Jahn-Teller coupling with e_2' vibrations and quadratic Jahn-Teller coupling with e_1' vibrations. In the $\widetilde{A}^2E''$ state of the nitrate radical, vibrations with e' symmetry have linear Jahn-Teller coupling and vibrations with either e' or e'' have quadratic Jahn-Teller coupling. More thorough discussions of linear versus quadratic Jahn-Teller effects are available elsewhere, however for simplicity Figure 2.1 provides a simple pictorial representation of the Jahn-Teller effect.[9,10]

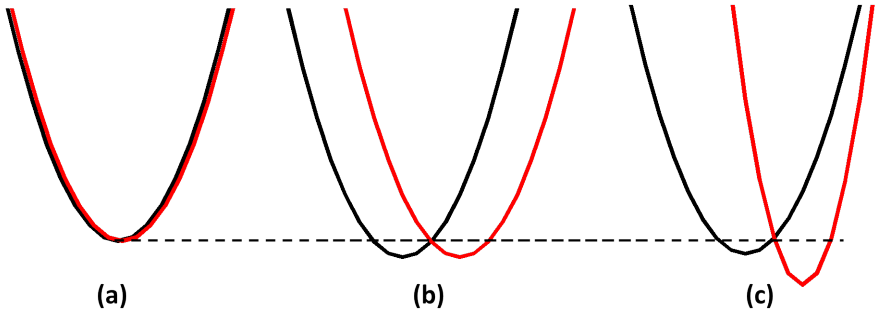

Figure 2.1: **(a)** Representation of a doubly degenerate electronic state **(b)** Linear Jahn-Teller effect splitting the previously degenerate electronic states symmetrically **(c)** Quadratic Jahn-Teller effects asymmetrically splitting previously degenerate electronic states.

Taking the nitrate radical as an example, whose triple-well potential energy surface in the $\widetilde{A}^2E''$ is presented in Figure 2.2. At the conical intersection where the upper and lower surfaces meet, the geometry can be considered as three equivalent N-O bonds in D_{3h} geometry. At the bottom of one of the triply degenerate wells, one N-O bond is either extended or contracted. At the height of the barriers between the three wells, one N-O bond is either shortened or extended. In either case, the molecule adopts C_{2v} symmetry.

With these nuclear geometric changes, the Born-Oppenheimer approximation breaks down. No longer are nuclear coordinates stationary, costing modern quantum chemistry

accuracy in predicting molecular and spectroscopic properties. In order to regain this accuracy, the magnitude of the Jahn-Teller distortion needs to be predicted computationally.

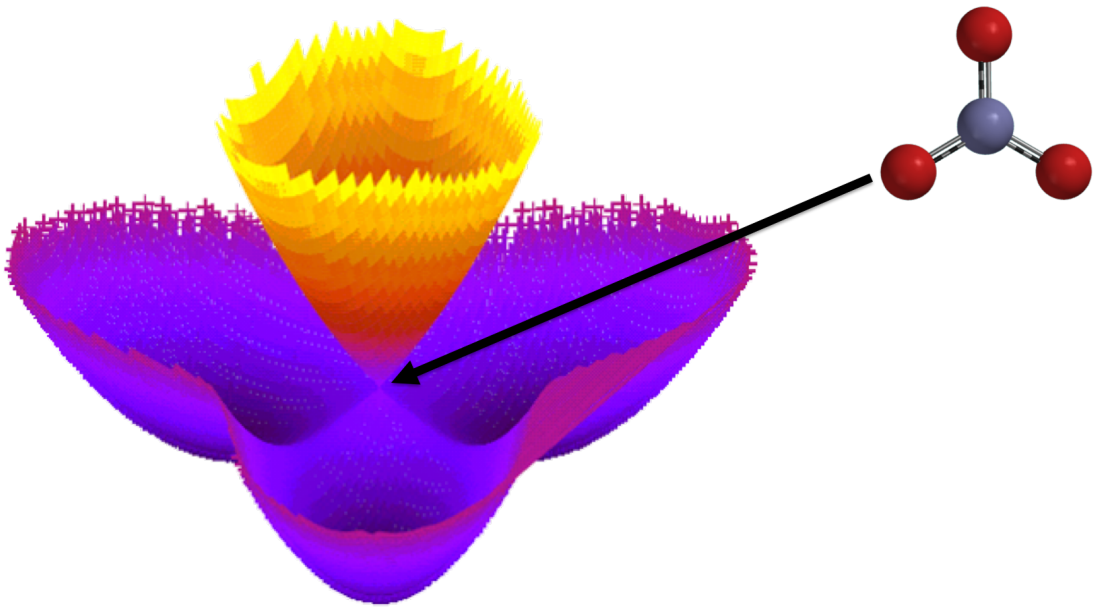

Figure 2.2: Calculated potential energy surface of nitrate radical. The undistorted geometry is found at the conical intersection between the upper and lower surface

2.3 The Watson Term

Nuclear geometry is readily measured via molecular rotations. The measured and predicted eigenenergies, E_N, are very sensitive to changes in geometry. The Jahn-Teller rotational Hamiltonian determines these energies including a term h_1, first derived by Watson, which gives an effective measure of Jahn-Teller distortions.[11] As the molecule travels around the lower moat of the distorted potential energy surface in Figure 2.2, an approximation to the

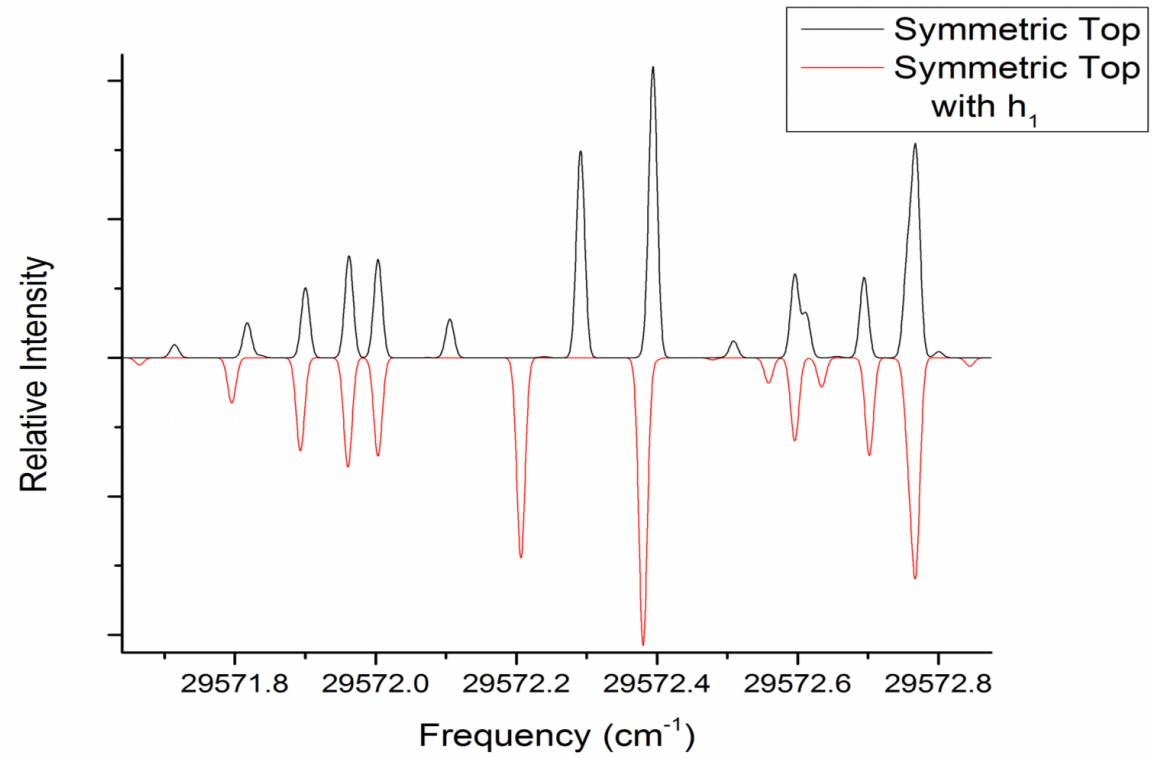

Figure 2.3: Simulations of $\widetilde{A}^2A_2'' \leftarrow \widetilde{X}^2E_1''$ 0_0^0 for cyclopentadienyl radical. Inclusion of h_1 alters the rotational structure of the transition.

rotational tensor is given by

$$\begin{pmatrix} B_{xx} - h_1 \cos\phi & h_1 \sin\phi & 0 \\ h_1 \sin\phi & B_{yy} + h_1 \cos\phi & 0 \\ 0 & 0 & B_{zz} \end{pmatrix} \tag{2.9}$$

where ϕ is a pseudo-rotation angle about the bottom of the moat. Figure 2.3 shows a simulation of the rotational structure of electronic transition from the ground to first excited state for the cyclopentadienyl radical both with and without the inclusion of the Watson term. Clearly, the inclusion of h_1 changes the rotational structure of this transition. The magnitude of h_1 can be determined by fitting experimental spectra, as was done by Liu et. al.[12]

2.3.1 Taylor Expanding Operators

h_1 is defined as

$$h_1 = \frac{1}{2} \langle \pm | \mathbf{B}_{\pm\pm} | \mp \rangle = \frac{1}{2} \langle E^{\kappa}_{s+} | \mathbf{B}_{++} | E^{\kappa}_{s-} \rangle + \frac{1}{2} \langle E^{\kappa}_{s-} | \mathbf{B}_{--} | E^{\kappa}_{s+} \rangle \tag{2.10}$$

Here, $|\pm\rangle$ represent the two components of a degenerate vibronic eigenstate corresponding to some Ψ which is an eigenfunction of both the electronic Hamiltonian and vibrational angular momentum, while with $\mathbf{B}_{\pm\pm}$ an electronic operator which acts on these functions. These degenerate states have $E^{k}_{s\pm}$ symmetry, where s can be 1 or 2, $\pm$ distinguishes between the $+$ and $-$ components of the degenerate state, and κ is either $\prime$ or $\prime\prime$ of the state. $\mathbf{B}_{\pm\pm}$ can be related to the Cartesian components of the rotational tensor as

$$\mathbf{B}_{\pm\pm} = \frac{1}{4} \left(B_{xx} - B_{yy} \mp 2iB_{xy} \right) \tag{2.11}$$

Similarly, the normal mode vibrations can be expressed in cylindrical coordinates as the two Cartesian components of that normal mode.

$$q_{\pm} = q_x \pm i q_y \tag{2.12}$$

At the conical intersection in the undistorted geometry, symmetry dictates $\mathbf{B}_{\pm\pm}$ as zero. However, $\mathbf{B}_{\pm\pm}$ has a non zero Taylor expansion when taken about the conical intersection, R_0, with respect to the normal modes of vibration.

$$\mathbf{B}_{\pm\pm} = \mathbf{B}_{\pm\pm}\Big|_{R_0} + \sum_{k} \sum_{r=+,-} \left(\frac{\partial \mathbf{B}_{\pm\pm}}{\partial q_{k,r}}\Big|_{R_0} q_{k,r} \right) + \frac{1}{2} \sum_{k} \sum_{m>k} \sum_{r_i=+,-} \sum_{r_j=+,-} \left(\frac{\partial^2 \mathbf{B}_{\pm\pm}}{\partial q_{k,r_i} \partial q_{l,r_j}}\Big|_{R_0} q_{k,r_i} q_{m,r_j} \right) + \ldots \tag{2.13}$$

Indexes k and m represent all Jahn-Teller active vibrational modes, and $r = +, -$ represents which component of the complex combination of states the derivatives are taken with respect to. Here, the Taylor series is truncated at the second order term, but higher orders are possible. Much of the remainder of this document will be focused upon the implementation of calculating the terms of Equation 2.13.

2.3.2 h_1' and h_1''

Revisiting the terms of the expansion, as stated previously at the conical intersection,

$$\mathbf{B}_{\pm\pm}\Big|_{R_0} = 0 \tag{2.14}$$

This can be seen through Equation 2.11. The principal axis system is chosen such that the plane of the molecule is defined as the xy plane and thus

$$\begin{aligned} B_{xx} &= B_{yy} \\ B_{xy} &= B_{yx} = 0 \end{aligned} \tag{2.15}$$

at which point and referencing Equation 2.11, Equation 2.14 becomes clear.

Inserting the first term of 2.13 into 2.10, we define

$$h_1' = \langle E_{s\pm}^k | \sum_k \sum_{r=+,-} \left(\frac{\partial \mathbf{B}_{\pm\pm}}{\partial q_{k,r}}\Big|_{R_0} q_{k,r} \right) | E_{s\mp}^k \rangle \tag{2.16}$$

Conveniently, the Taylor expansion has been done in way such that the derivatives of the rotational constant are no longer operators which act upon the vibronic eigenfunctions. As such we can remove the derivative from the integral to arrive at

$$h_1' = \frac{1}{2} \sum_i \sum_{r=+,-} \frac{\partial \mathbf{B}_{\pm\pm}}{\partial q_{k,r}}\Big|_{R_0} \langle E_{s\pm}^\kappa | \, q_{k,r} \, | E_{s\mp}^\kappa \rangle \tag{2.17}$$

There are two main components to this expression. The first being the derivative of the rotational constant. These are available via finite differencing and are the main focus of Chapter 3. The second is the expectation value of $q_{k,r}$, which are the ladder operators of the polar harmonic oscillator. These ladder operators act on vibronic calculated eigenfunctions and are the focus of Chapter 4.

Similarly, we define

$$h_1'' = \frac{1}{4} \sum_k \sum_{m>k} \sum_{r_i=+,-} \sum_{r_j=+,-} \frac{\partial^2 \mathbf{B}_{\pm\pm}}{\partial q_{k,r_i} \partial q_{l,r_j}}\Big|_{R_0} \langle E_{s\pm}^\kappa | \, q_{k,r_i} q_{m,r_j} \, | E_{s\mp}^\kappa \rangle \tag{2.18}$$

As before the only components to this expression are derivatives of the rotational constant and now higher orders of q applied to the same vibronic eigenfunctions.

h_1 has units of energy, which while expressible in many ways, will typically be presented as units of wavenumber, or inverse centimeters. In both of the derived expressions, $q_{k,\pm}$ and $|E^{\kappa}_{s\mp}\rangle$ are expressed in reduced normal coordinates, making the resulting matrix elements dimensionless. The rotational constant, $\mathbf{B}$, has units of energy, and thus derivatives taken with respect to a dimensionless quantity also have units of energy. Expressing $\mathbf{B}$ in units of wavenumber, as is conventional, produces h_1 quantities with proper units.

Of value is noting the applicability of this methodology to excited states. So long as vibronic eigenfunctions for any vibrationally excited state are available, values for h_1' and h_1'' can be calculated. Predicting values of h_1 for any excited state is useful in the identification of experimentally observed vibrational bands. In having accurate prediction of h_1, the rotational structure of vibrational transitions can be predicted, and thus features in vibrational spectra can be assigned to these Jahn-Teller active molecules.

To determine the derivatives of the rotational constant taken at the conical intersection, L-matrices for the normal vibrational modes of interest and the geometry at the conical intersection are needed.. Both of these are available via the CFOUR electronic structure package. The vibronic eigenfunctions are available via a software package called SOCJT 2 and require input parameters including harmonic frequency for vibrations and Jahn-Teller coupling constants, both of which are also available from CFOUR.[13] Thus, we have derived a method for predicting values of h_1 from exclusively theoretical methods. Alternatively, if the vibrational frequencies and Jahn-Teller couplings are found via experimental means, these parameters can be used in coordination with the derivatives of the rotational constant to calculate hybrid computational-experimental predictions for h_1 to test theory versus experiment.

Chapter 3
Derivatives Of The Rotational Constant

The first component of the expansion used to calculated h_1 is derivatives of the rotational constant. Matrix algebra is required to determine the proper derivatives needed to turn nuclear coordinated and displacements into proper derivatives as described by Equation 2.13. The method of finite differencing will be utilized to calculate these derivatives in Cartesian coordinates. Because the Taylor expansion is taken in polar coordinates, the transformation between coordinate systems is also required.

3.1 The Rotational Tensor

In general, the elements of the rotational tensor, $\mathbf{B}$ are defined

$$\mathbf{B_{ij}} = \frac{h}{8\pi^2 c}\mathbf{I_{ij}^{-1}} \tag{3.1}$$

where $\mathbf{I}$ is the inertial tensor. The elements of the inertial tensor are analytically known and in Cartesian coordinates take the form

$$\mathbf{I} = \begin{pmatrix} \sum_i \left(y_i^2 + z_i^2\right) m_i & -\sum x_i y_i m_i & -\sum x_i z_i m_i \\ -\sum y_i x_i m_i & \sum_i \left(x_i^2 + z_i^2\right) m_i & -\sum y_i z_i m_i \\ -\sum z_i x_i m_i & -\sum z_i y_i m_i & \sum_i \left(x_i^2 + y_i^2\right) m_i \end{pmatrix} \tag{3.2}$$

From this point forward, we will refer to these elements more concisely as

$$\mathbf{I} = \begin{pmatrix} I_{xx} & I_{xy} & I_{xz} \\ I_{yx} & I_{yy} & I_{yz} \\ I_{zx} & I_{zy} & I_{zz} \end{pmatrix} \tag{3.3}$$

The inverse, $\mathbf{A}^{-1}$ of a matrix $\mathbf{A}$ in general is given by

$$\mathbf{A}^{-1} = \frac{1}{\det \mathbf{A}} \mathrm{adj}\,(\mathbf{A}) \tag{3.4}$$

where adj is the adjugate matrix of $\mathbf{A}$ and det $\mathbf{A}$ is the determinant. This inverse is taken assuming the matrix is indeed invertible. In the case of the inertial tensor at the conical intersection, a non-zero determinant of $\mathbf{I}$ is a sufficient condition for invert-ability. The determinant of $\mathbf{I}$ is given by

$$\det \mathbf{I} = I_{xx}I_{yy}I_{zz} + I_{xy}I_{yz}I_{zx} + I_{xz}I_{yx}I_{zy} - I_{xz}I_{yy}I_{zx} - I_{xx}I_{yz}I_{zy} - I_{xy}I_{yx}I_{zz} \tag{3.5}$$

However, at the conical intersection, the determinant reduces simply to

$$\det \mathbf{I} = I_{xx}I_{yy}I_{zz} \tag{3.6}$$

as all off diagonal elements are zero in the principal axis system. Clearly this term is nonzero as none of the diagonal elements of the inertial tensor can be zero for a real molecule.

Specifically, the elements of interest in Equation 2.11 in our coordinate system are

$$B_{xx} = \frac{h}{8\pi^2 c}\frac{1}{\det \mathbf{I}}(I_{yy}I_{zz} - I_{yz}I_{zy}) = \frac{h}{8\pi^2 c} I_{xx}^{-1} \tag{3.7a}$$

$$B_{yy} = \frac{h}{8\pi^2 c}\frac{1}{\det \mathbf{I}}(I_{xx}I_{zz} - I_{xz}I_{zx}) = \frac{h}{8\pi^2 c} I_{yy}^{-1} \tag{3.7b}$$

$$B_{xy} = \frac{h}{8\pi^2 c}\frac{1}{\det \mathbf{I}}(I_{xz}I_{zy} - I_{xy}I_{zz}) = \frac{h}{8\pi^2 c} I_{xy}^{-1} \tag{3.7c}$$

where again the fact that all off diagonal elements are zero in our axis system in order to simplify the expressions.

3.2 First Derivatives

First, lets start with the definition of inverse matrices.

$$\mathbf{I} \cdot \mathbf{I^{-1}} = \mathbf{I_n} \tag{3.8}$$

where $\mathbf{I_n}$ is the identity matrix. Differentiating this expression with respect to some vibrational normal coordinate, q_a, yields

$$\mathbf{I} \cdot \frac{\partial \mathbf{I^{-1}}}{\partial q_a} + \frac{\partial \mathbf{I}}{\partial q_a} \cdot \mathbf{I^{-1}} = 0 \tag{3.9}$$

From here we see that

$$\frac{\partial \mathbf{I^{-1}}}{\partial q_a} = -\mathbf{I^{-1}} \cdot \frac{\partial \mathbf{I}}{\partial q_a} \cdot \mathbf{I^{-1}} \tag{3.10}$$

Utilizing Equation 3.1, we now reach an easily accessible way to determine the elements of the first derivatives of the rotational tensor in Cartesian coordinates through derivatives of the inertial tensor through

$$\frac{\partial \mathbf{B}}{\partial q_a} = \frac{h}{8\pi^2 c} \frac{\partial \mathbf{I^{-1}}}{\partial q_a} = -\frac{h}{8\pi^2 c} \mathbf{I^{-1}} \cdot \frac{\partial \mathbf{I}}{\partial q_a} \cdot \mathbf{I^{-1}} \tag{3.11}$$

3.2.1 Finite Differencing

Derivatives can be taken by utilizing the method of finite differencing,

$$\frac{\partial \mathbf{I}}{\partial q_a} \approx \frac{\mathbf{I}(\omega + \delta q_a) - \mathbf{I}(\omega - \delta q_a)}{2\delta} \tag{3.12}$$

where ω reprsents the equilibrium geometry and δq_a is a small, finite movement taken along some normal vibrational mode q_a. More precisely these derivatives can be expanded by utilizing a uniform grid of spacing along a single mode and including these higher order terms of the grid with appropriate coefficients as given in Table 3.1. Further expanding the grid gives more accurate determinations of the derivatives. The grid is generated by taking consecutive steps of uniform size in both forward and reverse directions. For all first derivatives, the grid is generated up to third order. Accuracy improvements beyond second order are typically negligible within computer round off.

Table 3.1: Coefficients for first derivative central finite differentiation using a uniform grid

Steps Along Grid	**-3**	**-2**	**-1**	**0**	**1**	**2**	**3**
Coefficient			-1/2	0	1/2		
		1/12	-2/3	0	2/3	-1/12	
	-1/60	3/20	-3/4	0	3/4	-3/20	1/60

3.3 Higher Order Derivatives

It is advantageous to express the derivatives of the rotational constant in terms of derivatives of the inertial tensor for higher order derivatives. The general approach taken in the previous section for first derivatives can be easily extended to second derivatives of the rotational constant in terms of second derivatives of the inertial tensor. Starting with Equation 3.9, differentiation with respect to a second vibrational normal mode, q'' yields

$$\frac{\partial \mathbf{I}}{\partial q''}\frac{\partial \mathbf{I^{-1}}}{\partial q'} + \mathbf{I}\frac{\partial^2 \mathbf{I^{-1}}}{\partial q'' \partial q'} + \frac{\partial^2 \mathbf{I}}{\partial q'' \partial q'}\mathbf{I^{-1}} + \frac{\partial \mathbf{I}}{\partial q'}\frac{\partial \mathbf{I^{-1}}}{\partial q''} = 0 \tag{3.13}$$

Here, q' and q'' refer to any two vibrational modes, which can be the same or different. Rearranging and left multiplying by the inverse inertial tensor yields

$$\frac{\partial^2 \mathbf{I^{-1}}}{\partial q'' \partial q'} = -\mathbf{I^{-1}}\frac{\partial \mathbf{I}}{\partial q''}\frac{\partial \mathbf{I^{-1}}}{\partial q'} - \mathbf{I^{-1}}\frac{\partial \mathbf{I}}{\partial q'}\frac{\partial \mathbf{I^{-1}}}{\partial q''} - \mathbf{I^{-1}}\frac{\partial^2 \mathbf{I}}{\partial q'' \partial q'}\mathbf{I^{-1}} \tag{3.14}$$

Finally, utilizing Equation 3.10, we arrive at what will be our most useful expression of second derivatives of the rotational constant in the Cartesian basis of

$$\frac{\partial^2 \mathbf{B}}{\partial q'' \partial q'} \Big/ \frac{h}{8\pi^2 c} = \frac{\partial^2 \mathbf{I^{-1}}}{\partial q'' \partial q'} = \mathbf{I^{-1}}\frac{\partial \mathbf{I}}{\partial q''}\mathbf{I^{-1}}\frac{\partial \mathbf{I}}{\partial q'}\mathbf{I^{-1}} + \mathbf{I^{-1}}\frac{\partial \mathbf{I}}{\partial q'}\mathbf{I^{-1}}\frac{\partial \mathbf{I}}{\partial q''}\mathbf{I^{-1}} - \mathbf{I^{-1}}\frac{\partial^2 \mathbf{I}}{\partial q'' \partial q'}\mathbf{I^{-1}} \tag{3.15}$$

3.3.1 Higher Order Finite Differencing

In order to determine the second derivatives of the rotational constant from Equation 3.15, the inertial tensor first derivatives with respect to each vibrational normal coordinate have previously been tabulated via finite differencing, the inverse inertial tensor is readily available analytically, leaving the second derivative of the inertial tensor the only remaining quantity to be tabulated. Fortunately, finite differencing is still available for higher or-

der derivatives. For diagonal second derivatives–i.e. second derivatives taken with respect to a single vibrational mode–are available via Equation high orders of accuracy are again available from uniform grid generation with coefficients according to Table 3.2.

$$\frac{\partial^2 \mathbf{I}}{\partial q' \partial q'} = \frac{\mathbf{I}(\omega + \delta q') - 2\mathbf{I}(\omega) + \mathbf{I}(\omega - \delta q'}{\delta^2} \tag{3.16}$$

with ω again representing the reference geometry and $\delta q'$ is a small finite movement taken along some normal vibrational mode q'. In practice, there is a lower bound on the size of step taken along these modes due to limits within storage of a signed double. Again, these derivatives were taken up to third order accuracy, however there was negligible improvement over even first order grid spacing in this case.

For mixed second derivatives, a two dimensional grid is generated, taking steps along each of the respective vibrational modes. The mixed derivatives have the form

$$\frac{\partial^2 \mathbf{I}}{\partial q'' \partial q'} = \frac{\mathbf{I}(\omega + \delta q'' + \delta q') - \mathbf{I}(\omega - \delta q'' + \delta q') - \mathbf{I}(\omega + \delta q'' - \delta q') + \mathbf{I}(\omega - \delta q'' - \delta q')}{4\delta^2} \tag{3.17}$$

Table 3.2: Coefficients for second derivative central finite differentiation using a uniform grid

Steps Along Grid	**-3**	**-2**	**-1**	**0**	**1**	**2**	**3**
Coefficient			1	-2	1		
		-1/12	4/3	-5/2	4/3	-1/12	
	1/90	-3/20	3/2	-49/18	3/2	-3/20	1/90

3.4 Complex Combinations

In the case of the SOCJT basis, it is most convenient to express the two components of the k^{th} degenerate vibrational mode, denoted as q_{ka} and q_{kb}, in the form of

$$q_{k\pm} = q_{ka} \pm i q_{kb} \tag{3.18}$$

It will become important to express the derivatives of the rotational constant in this cylindrical coordinate system. The explicit derivation for the first derivative coordinate system relations is presented here.

3.4.1 First Derivative Relations

We begin by explicitly expressing the two components of the complex combinations

$$q_{k+} = (q_{ka} + iq_{kb}) \tag{3.19}$$

$$q_{k-} = (q_{ka} - iq_{kb}) \tag{3.20}$$

and then rewrite these in terms of the two degenerate components of the oscillator

$$q_{ka} = \frac{1}{2}(q_{k+} + q_{k-}) \tag{3.21}$$

$$q_{kb} = \frac{1}{2i}(q_{k+} - q_{k-}) \tag{3.22}$$

Now we utilize the chain rule to get

$$\frac{\partial B_{\pm\pm}}{\partial q_{k\pm}} = \frac{\partial B_{\pm\pm}}{\partial q_{ka}}\frac{\partial q_{ka}}{\partial q_{\pm}} + \frac{\partial B_{\pm\pm}}{\partial q_{kb}}\frac{\partial q_{kb}}{\partial q_{\pm}} \tag{3.23a}$$

$$\frac{\partial B_{\pm\pm}}{\partial q_{k\pm}} = \frac{1}{2}\frac{\partial B_{\pm\pm}}{\partial q_{ka}} \pm \frac{1}{2i}\frac{\partial B_{\pm\pm}}{\partial q_{kb}} \tag{3.23b}$$

which we further expand to more explicitly arrive at

$$\begin{aligned}\frac{\partial B_{\pm\pm}}{\partial q_{k+}} =& \frac{\partial B_{\pm\pm}}{\partial q_{ka}}\frac{\partial q_{ka}}{\partial q_{k+}} + \frac{\partial B_{\pm\pm}}{\partial q_{kb}}\frac{\partial q_{kb}}{\partial q_{k+}} \\ =& \frac{1}{2}\frac{\partial B_{\pm\pm}}{\partial q_{ka}} + \frac{1}{2i}\frac{\partial B_{\pm\pm}}{\partial q_{kb}}\end{aligned} \tag{3.24a}$$

$$\begin{aligned}\frac{\partial B_{\pm\pm}}{\partial q_{k-}} =& \frac{\partial B_{\pm\pm}}{\partial q_{ka}}\frac{\partial q_{ka}}{\partial q_{k-}} + \frac{\partial B_{\pm\pm}}{\partial q_{kb}}\frac{\partial q_{kb}}{\partial q_{k-}} \\ =& \frac{1}{2}\frac{\partial B_{\pm\pm}}{\partial q_{ka}} - \frac{1}{2i}\frac{\partial B_{\pm\pm}}{\partial q_{kb}}\end{aligned} \tag{3.24b}$$

Reinserting the definitions of $B_{\pm\pm}$ in terms of the elements of the rotational tensor.

$$\begin{aligned}\frac{\partial B_{\pm\pm}}{\partial q_{k+}} =& \frac{1}{8}\left(\frac{\partial(B_{xx}-B_{yy}\mp 2iB_{xy})}{\partial q_a}\right)+\frac{1}{8i}\left(\frac{\partial(B_{xx}-B_{yy}\mp 2iB_{xy})}{\partial q_b}\right)\\ =& \frac{1}{8}\left(\frac{\partial B_{xx}}{\partial q_a}-\frac{\partial B_{yy}}{\partial q_a}\mp 2i\frac{\partial B_{xy}}{\partial q_a}\right)+\frac{1}{8i}\left(\frac{\partial B_{xx}}{\partial q_b}-\frac{\partial B_{yy}}{\partial q_b}\mp 2i\frac{\partial B_{xy}}{\partial q_b}\right)\end{aligned} \tag{3.25a}$$

$$\begin{aligned}\frac{\partial B_{\pm\pm}}{\partial q_{k-}} =& \frac{1}{8}\left(\frac{\partial(B_{xx}-B_{yy}\mp 2iB_{xy})}{\partial q_a}\right)-\frac{1}{8i}\left(\frac{\partial(B_{xx}-B_{yy}\mp 2iB_{xy})}{\partial q_b}\right)\\ =& \frac{1}{8}\left(\frac{\partial B_{xx}}{\partial q_a}-\frac{\partial B_{yy}}{\partial q_a}\mp 2i\frac{\partial B_{xy}}{\partial q_a}\right)-\frac{1}{8i}\left(\frac{\partial B_{xx}}{\partial q_b}-\frac{\partial B_{yy}}{\partial q_b}\mp 2i\frac{\partial B_{xy}}{\partial q_b}\right)\end{aligned} \tag{3.25b}$$

Now we utilize the symmetry relations that[14]

$$\frac{\partial B_{xx}}{\partial q_a} = -\frac{\partial B_{yy}}{\partial q_a} = \frac{\partial B_{xy}}{\partial q_b} \tag{3.26}$$

$$\frac{\partial B_{xx}}{\partial q_b} = \frac{\partial B_{yy}}{\partial q_b} = \frac{\partial B_{xy}}{\partial q_a} = 0 \tag{3.27}$$

for a five fold rotational axis to first remove zero terms

$$\frac{\partial B_{\pm\pm}}{\partial q_{k+}} = \frac{1}{8}\left(\frac{\partial B_{xx}}{\partial q_a}-\frac{\partial B_{yy}}{\partial q_a}\mp 2\frac{\partial B_{xy}}{\partial q_b}\right) \tag{3.28a}$$

$$\frac{\partial B_{\pm\pm}}{\partial q_{k-}} = \frac{1}{8}\left(\frac{\partial B_{xx}}{\partial q_a}-\frac{\partial B_{yy}}{\partial q_a}\pm 2\frac{\partial B_{xy}}{\partial q_b}\right) \tag{3.28b}$$

and then reducing further to

$$\frac{\partial B_{\pm\pm}}{\partial q_{k+}} = \frac{1}{8}\left(2\frac{\partial B_{xx}}{\partial q_a}\mp 2\frac{\partial B_{xy}}{\partial q_b}\right) \tag{3.29a}$$

$$\frac{\partial B_{\pm\pm}}{\partial q_{k-}} = \frac{1}{8}\left(2\frac{\partial B_{xx}}{\partial q_a}\pm 2\frac{\partial B_{xy}}{\partial q_b}\right) \tag{3.29b}$$

Expanding out further we obtain

$$\frac{\partial B_{++}}{\partial q_{k+}} = \frac{1}{8}\left(2\frac{\partial B_{xx}}{\partial q_a}-2\frac{\partial B_{xy}}{\partial q_b}\right) \tag{3.30a}$$

$$\frac{\partial B_{--}}{\partial q_{k+}} = \frac{1}{8}\left(2\frac{\partial B_{xx}}{\partial q_a}+2\frac{\partial B_{xy}}{\partial q_b}\right) \tag{3.30b}$$

$$\frac{\partial B_{++}}{\partial q_{k-}} = \frac{1}{8}\left(2\frac{\partial B_{xx}}{\partial q_a} + 2\frac{\partial B_{xy}}{\partial q_b}\right) \tag{3.30c}$$

$$\frac{\partial B_{--}}{\partial q_{k-}} = \frac{1}{8}\left(2\frac{\partial B_{xx}}{\partial q_a} - 2\frac{\partial B_{xy}}{\partial q_b}\right) \tag{3.30d}$$

which finally this reduces down to the forms of

$$\frac{\partial B_{--}}{\partial q_{k-}} = \frac{1}{2}\frac{\partial B_{xx}}{\partial q_a} \tag{3.31a}$$

$$\frac{\partial B_{++}}{\partial q_{k+}} = \frac{1}{2}\frac{\partial B_{xx}}{\partial q_a} \tag{3.31b}$$

$$\frac{\partial B_{++}}{\partial q_{k-}} = \frac{\partial B_{--}}{\partial q_{k+}} = 0 \tag{3.31c}$$

A similar analysis can be done in the case of a three fold rotational axis as for the nitrate radical in order to achieve

$$\frac{\partial B_{--}}{\partial q_{k+}} = \frac{1}{2}\frac{\partial B_{xx}}{\partial q_a} \tag{3.32a}$$

$$\frac{\partial B_{++}}{\partial q_{k-}} = \frac{1}{2}\frac{\partial B_{xx}}{\partial q_a} \tag{3.32b}$$

$$\frac{\partial B_{++}}{\partial q_{k+}} = \frac{\partial B_{--}}{\partial q_{k-}} = 0 \tag{3.32c}$$

It is important to note that all symmetry relations and derivatives are taken as part of the Taylor expansion about the conical intersection where the geometry is undistorted.

3.4.2 Second Derivative Relations

Similar analysis can be done for the second derivatives in the cylindrical basis. Similarly to before, we begin by noting

$$q'_{r_i} = q'_a + (-1)^{n_i} i q'_b \tag{3.33}$$

which is an equivalent expression to 3.18. The factor n_i takes the value of 0 for $r_i = +$ and 1 for $r_i = -$. Noting that

$$\frac{\partial q'_a}{\partial q'_{r_i}} = \frac{1}{2} \tag{3.34a}$$

$$\frac{\partial q'_k}{\partial q'_{r_i}} = \frac{(-1)^{n_i}}{2} i \tag{3.34b}$$

we expand completely to reach

$$\begin{aligned}
\frac{\partial^2 B_{\pm\pm}}{\partial q'_{r_i} \partial q''_{r_j}} =& \frac{1}{16}\left(\frac{\partial^2 B_{xx}}{\partial q'_a \partial q''_b} + (-1)^{n_i+1} i \frac{\partial^2 B_{xx}}{\partial q'_b \partial q''_a} + (-1)^{n_j+1} i \frac{\partial^2 B_{xx}}{\partial q'_a \partial q''_b} + (-1)^{n_i+n_j+1} \frac{\partial^2 B_{xx}}{\partial q'_b \partial q''_b}\right) \\
& - \frac{1}{16}\left(\frac{\partial^2 B_{yy}}{\partial q'_a \partial q''_b} + (-1)^{n_i+1} i \frac{\partial^2 B_{yy}}{\partial q'_b \partial q''_a} + (-1)^{n_j+1} i \frac{\partial^2 B_{yy}}{\partial q'_a \partial q''_b} + (-1)^{n_i+n_j+1} \frac{\partial^2 B_{yy}}{\partial q'_b \partial q''_b}\right) \\
& \pm \frac{1}{8}\left(-i \frac{\partial^2 B_{xy}}{\partial q'_a \partial q''_a} + (-1)^{n_i+1} \frac{\partial^2 B_{xy}}{\partial q'_b \partial q''_a} + (-1)^{n_j+1} \frac{\partial^2 B_{xy}}{\partial q'_a \partial q''_b} - (-1)^{n_i+n_j+1} i \frac{\partial^2 B_{xx}}{\partial q'_b \partial q''_b}\right)
\end{aligned} \tag{3.35}$$

In this expansion, we leave the imaginary terms written for completeness. However, because h_1 is a real quantity, all of the terms of the Taylor expansion must also be real. The imaginary terms ultimately cancel via symmetry, leaving the second derivative of the rotational constant as an entirely real value as expected.

3.5 Implementation

The derivatives and their transformation between coordinate systems is all done systematically via code written in MATLAB. MATLAB was chosen to best handle explicit matrix multiplication of equations such as 3.15. The input to the program requires the number of atoms, the masses of the respective atoms in Daltons, and a text file containing the L-Matrices for all $3N - 6$ vibrations as well as the reference geometry at the conical intersection, $\mathbf{R_0}$. The input file is available via electronic structure methods to be discussed in the next chapter. Further documentation is encapsulated within the code.

Chapter 4
Vibronic Eigenfunctions

The second component of the expansion used to calculated h_1 is the matrix elements of $q_{\pm}$. In order to calculate these matrix elements, vibronic eigenfunctions are calculated via software named SOCJT 2–an acronym for the second iteration of **S**pin **O**rbit **C**oupling and **J**ahn-**T**eller; pronounced *"sock-it"*. The eigenfunctions produced as a result are readily available for determination of matrix elements, in this case the contribution to h_1.

4.1 SOCJT 2

SOCJT 2 diagonalizes the spin-vibronic portion of the Jahn-Teller Hamiltonian, resulting in eigenvalues and eigenvectors of these vibronic states. As discussed in Chapter 2, the exact wave function for a system is often unavailable. Commonly, the wavefunction is expressed as linear combinations of basis functions,

$$\Psi_i = \sum_j c_{ij}\phi_j \tag{4.1}$$

or equivalently

$$|\Psi_i\rangle = \sum_j c_{ij}\,|\phi_j\rangle \tag{4.2}$$

In SOCJT 2, the spin vibronic problem utilizes a basis of the form

$$|\phi\rangle = |\text{Electronic}\rangle\,|\text{Vibrational}\rangle\,|\text{Spin}\rangle \tag{4.3}$$

Specifically, an eigenfunction can be expressed as

$$|E^{\kappa}_{s,\pm}\rangle \equiv |\pm j, n_j, E^{\kappa}_s, \Sigma\rangle = \sum_i \left(c_{i,n_j,\Sigma} |\Lambda_i\rangle \prod_{m=1}^{p} |v_{m,i}, l_{m,i}\rangle \prod_{n=1}^{3N-6-2p} |v_i\rangle |\Sigma_i\rangle \right) \tag{4.4}$$

where E^{κ}_s is the symmetry of the vibronic eigenfunction, $\pm j$ distinguishes between the + and − components of a degenerate state, n_j indexes which eigenvector within a given j symmetry block the state is, and Σ is the spin component. The basis is composed of $\pm\Lambda$ indicating one of the two degenerate electronic components, p degenerate vibrational modes expressed as polar harmonic oscillators with principal quantum number v_i and angular momentum l_i, $3N-6-2p$ non-degenerate vibrational modes expressed as harmonic oscillators, and a coefficient $c_{i,n_j,\Sigma}$ specific to the eigenstate. The spin component is only relevant in the case of spin orbit coupling, and thus since spin orbit coupling is not incorporated into calculations contributing to h_1, Equation 4.4 can be expressed as

$$|E^{\kappa}_{s,\pm}\rangle \equiv |\pm j, n_j, E^{\kappa}_s\rangle |\Sigma\rangle = \sum_i \left(c_{i,n_j,\Sigma} |\Lambda_i\rangle \prod_{m=1}^{p} |v_{m,i}, l_{m,i}\rangle \prod_{n=1}^{3N-6-2p} |v_i\rangle \right) |\Sigma\rangle \tag{4.5}$$

SOCJT 2 has been extensively tested and utilized in other studies of Jahn-Teller active molecules.[15,13,16] More detailed information on SOCJT 2, including algorithmic considerings definitions of j in the chosen basis, capabilities and limitations, is available elsewhere.[9,13] Here, only the information pertinent to determining h_1 is presented.

4.2 Jahn-Teller Parameters and SOCJT 2 Input

In order to build a complete basis and Hamiltonian matrix for SOCJT 2 to determine eigenvectors and eigenvalues of Jahn-Teller vibronic states, SOCJT 2 requires information about the vibrational modes. For Jahn-Teller active modes, the required values are the harmonic vibrational frequency, ω, and any Jahn-Teller coupling parameters, D and K.

The harmonic frequency and Jahn-Teller coupling constants are defined as

$$\omega_i = \frac{1}{2\pi c}\left(\frac{\lambda_i}{M_i}\right)^{1/2} \tag{4.6}$$

$$D_i = \frac{k_i^2}{2\hbar}\left(\frac{M_i}{\lambda_i^3}\right)^{1/2} \tag{4.7}$$

$$K_i = \frac{g_{ii}}{\lambda_i} \tag{4.8}$$

where M_i is the reduced mass of vibrational mode i, λ_i is the harmonic force constant of the vibrational mode, k_i is the linear JT coupling constant, and g_{ii} is the quadratic JT coupling constant. Briefly, λ_i, k_i, and g_{ii} are available via electronic structure methods

$$\lambda_i = \frac{\partial^2(\langle\Lambda_\pm|\,\hat{\mathcal{H}}_e\,|\Lambda_\pm\rangle)_0}{\partial q_{i,+}\partial q_{i,-}} \tag{4.9a}$$

$$k_i = \frac{\partial(\langle\Lambda_\pm|\,\hat{\mathcal{H}}_e\,|\Lambda_\mp\rangle)_0}{\partial q_{i,\pm}} \tag{4.9b}$$

$$g_{ii} = \frac{\partial^2(\langle\Lambda_\pm|\,\hat{\mathcal{H}}_e\,|\Lambda_\mp\rangle)_0}{\partial q_{i,\pm}\partial q_{i,\pm}} \tag{4.9c}$$

where $\hat{\mathcal{H}}_e$ is the electronic Hamiltonian acting on the electronic potential energy surface.

4.2.1 Electronic Structure Calculations

The CFOUR electronic structure package is used to calculate *ab initio* vibrational parameters and Jahn-Teller coupling constants. For radical molecules, two routes are generally available toward completing these calculations, Equation of Motion Ionization Potential (EOMIP) and Equation of Motion Electron Affinity (EOMIP). The ionization potential method utilizes the anionic analogue to the radical molecule and then removes an electron to reach the radical. For example, for the cyclopentadienyl radical C_5H_5, this method would calculate a geometry and parameters based upon $C_5H_5^-$. The electron affinity method works similarly, however uses the cationic species for reference. In the example previously, $C_5H_5^+$ would be used.

The electronic structure calculations were provided via collaborative efforts with Dr.

John Stanton at the University of Florida. The calculations are done using CCSD/EOMIP. The derivatives calculated in Chapter 3 utilized normal mode vibrations and reference geometries of the anionic compound.

4.2.2 SOCJT 2 Output and Limitations

SOCJT 2 produces eigenvalues and eigenvectors. The eigenvalues and eigenfunctions are organized by their j value. In the case of linear only Jahn-Teller coupling, j is a good quantum number defining symmetry blocks. However, in the case of quadratic Jahn-Teller coupling, j is not a good quantum number, but is used to distinguish E type and A type symmetric levels.

Each eigenvalue can be output with its corresponding eigenfunction. The eigenfunction is displayed as written in Equation 4.2. Generally, only a few basis functions contribute significantly to the total eigenfunction. In this case, only the basis functions with normalized coefficients, $c_{i,j}$, greater than some cutoff value, typically 0.00001, are displayed. Sample output is provided in Figure 4.1

4.3 Ladder Operators

The derived relations toward calculating h_1 rely upon $q_{k,\pm}$, which are the ladder operators on the polar harmonic oscillator. They are called the ladder operators in that they 'walk' one vibrational level up and down possible vibrational states, analogous to climbing or descending a ladder's rungs. The way the ladder operators act upon the polar harmoic oscillator basis can be expressed succinctly as[17]

$$q_{\pm}^{n}\left|v,l\right\rangle = (2\gamma)^{-n/2}\sum_{m=0}^{n}\left[\binom{n}{m}\prod_{h=1-m}^{n-m}\left(v \pm \sigma_h l + 2h\right)^{1/2}\right]\left|v+n-2m, l\pm n\right\rangle \tag{4.10}$$

$$\sigma_h = \begin{cases} 1 & h > 0 \\ -1 & h \leq 0 \end{cases}$$

where n being the number of times the operator is applied. As mentioned in Chapter 2, dimensionless reduced normal coordinates are used for the polar harmonic oscillators. In

```
Eigenvalue 1 = -4496.0158

Eigenvector: (Only vectors with coefficients larger than 0.1 are shown)


Coefficient v(1) l(1) v(2) l(2) lambda
 -0.125926   0    0    2   -2   -1
  0.149059   0    0    3   -3    1
 -0.201217   0    0    4   -2   -1
  0.194645   0    0    5   -3    1
 -0.199012   0    0    6   -2   -1
  0.168118   0    0    7   -3    1
 -0.148091   0    0    8   -2   -1
  0.113444   0    0    9   -3    1
 -0.163008   0    0    1    1   -1
  0.232706   0    0    2    0    1
 -0.268804   0    0    3    1   -1
  0.287202   0    0    4    0    1
 -0.275230   0    0    5    1   -1
  0.251192   0    0    6    0    1
 -0.212858   0    0    7    1   -1
```

Figure 4.1: Sample SOCJT 2 output for a vibrationally excited state of a system with two degenerate vibrational modes. The eigenvalue of the state is listed first as the eigenvalue. The quantum numbers for v and l for each degenerate vibrational mode as well as the electronic component, Λ, are displayed. The Coefficient column is the individual eigenvector's (represented by a single row of output) contribution to the overall state.

this case

$$\gamma = 1 \tag{4.11}$$

4.3.1 Expectation Values

The required calculation to determine h_1 is to determine the matrix elements of $q_\pm$ between the two components of the degenerate state. SOCJT 2 arbitrarily makes a choice to calculate either the $+j$ or $-j$ component of the degenerate states, however the complimentary degenerate component is readily available for a given state

$$|E^\kappa_{s+}\rangle = \sum_i c_i \, |\Lambda_i\rangle \prod_{m=1}^{p} |v_{m,i}, l_{m,i}\rangle \tag{4.12}$$

via the relation[9]

$$|E^\kappa_{s-}\rangle = \sum_i c_i \, |-\Lambda_i\rangle \prod_{m=1}^{p} |v_{m,i}, -l_{m,i}\rangle \tag{4.13}$$

Where any spin or non-degenerate components of the basis not explicit written are assumed to be delta functions. As an explicit example, for the first order term of the Taylor expansion the matrix elements take the form

$$\langle E^\kappa_{s+}| \, q_+ \, \langle E^\kappa_{s-}| = \sum_a c^*_a \, \langle \Lambda_a| \prod_{n=1}^{p} \langle v_{n,a}, l_{n,a}| \, (q_+) \sum_b c^*_b \, |\Lambda_b\rangle \prod_{m=1}^{p} |v_{m,b}, l_{m,b}\rangle \tag{4.14a}$$

$$= \sum_a \sum_b c^*_a c_b \, \langle \Lambda_a| \, |\Lambda_b\rangle \prod_{n=1}^{p} \langle v_{n,a}, l_{n,a}| \, (q_+) \prod_{m=1}^{p} |v_{m,b}, l_{m,b}\rangle \tag{4.14b}$$

$$\begin{aligned} &= \sum_a \sum_b c^*_a c_b \delta_{\Lambda_a,\Lambda_b} \sqrt{\frac{v_{m,b} + l_{m,b} + 2}{2}} \delta_{v_{m,b}+1,v_{n,a}} \delta_{l_{m,b}+1,l_{n,a}} \prod_{n' \neq n}^{p} \prod_{m' \neq m}^{p} \delta_{v_{m'},v_{n'}} \delta_{l_{m'},l_{n'}} \\ &+ \sum_a \sum_b c^*_a c_b \delta_{\Lambda_a,\Lambda_b} \sqrt{\frac{v_{m,b} - l_{m,b}}{2}} \delta_{v_{m,b}-1,v_{n,a}} \delta_{l_{m,b}+1,l_{n,a}} \prod_{n' \neq n}^{p} \prod_{m' \neq m}^{p} \delta_{v_{m'},v_{n'}} \delta_{l_{m'},l_{n'}} \end{aligned} \tag{4.14c}$$

4.4 Implementation

Multiple iterations of code have been written in order to calculate these matrix elements. Issues of calculation run time have been extensively considered, with early iterations of

matrix element calculations taking significant computational power to run. Currently, the most optimized version is a GUI developed by Dr. Ketan Sharma, which reduced the run time to a matter of seconds to calculate matrix elements for large numbers of vibrational states, in practice up to 40 vibrational states in only a few seconds.

Extensive testing has been done comparing the calculated values of $q_{\pm}$ in the cylindrical basis versus calculations of q_x and q_y in the Cartesian basis done by Dr. John Stanton. The relationships between the matrix elements in the Cartesian basis and the cylindrical basis can be found by expansion of the transformation between coordinate systems. For example, utilizing the definitions of

$$q_{\pm} = q_x \pm i q_y \tag{4.15a}$$

$$|\Psi_{\pm}\rangle = \frac{1}{\sqrt{2}} \left[|\Psi_x\rangle \pm i \, |\Psi_y\rangle \right] \tag{4.15b}$$

$$\langle \Psi_{\pm}| = \frac{1}{\sqrt{2}} \left[\langle \Psi_x| \mp i \, \langle \Psi_y| \right] \tag{4.15c}$$

one can show that

$$\langle E_+| \, q_+ \, |E_-\rangle + \langle E_-| \, q_- \, |E_+\rangle = 4 \, \langle \Psi_x| \, q_x \, |\Psi_x\rangle \tag{4.16}$$

It is important to note that the complex combinations of wavefunctions from the Cartesian basis to the cylindrical basis utilizes normalized combinations, however the complex combinations of q operators are unnormalized.

Chapter 5
Cyclopentadienyl Results

5.1 The Molecule

The cyclopentadienyl radical has been studied for more than half a century–the first absorption spectra was taken in 1956.[18] Cyclopentadienyl has been an ideal candidate for studying Jahn-Teller effects in that its ground electronic state is doubly degenerate and group theoretically available for Jahn-Teller distortions. Electron Paramagnetic Resonance Spectroscopy, Laser Induced Fluorescence, Rotational Vibrational spectroscopy methods have all been utilized to probe geometric distortions from the predicted equilibrium structure predicted in Figure 5.1 with D_{5h} symmetry.[19,5,20,21,22,23]

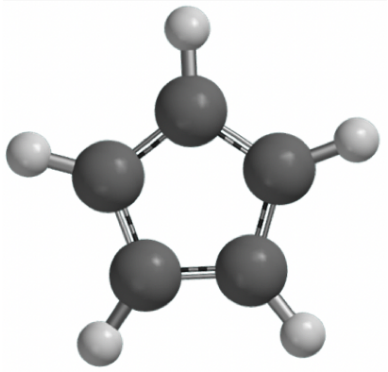

Figure 5.1: Predicted geometry of cyclopentadienyl radical at the conical intersection with five equivalent Carbon-Carbon and five equivalent Carbon-Hydrogen bonds.

5.1.1 Electronic Structure Parameters

Symmetries, harmonic force constants and vibrational frequencies, and linear and quadratic Jahn-Teller coupling constants where applicable were determined via CFOUR calculations. These results are presented in Table 5.1.

Group theoretically, e_2' vibrations are only linearly Jahn-Teller active where as e_1' vibrations are only quadratically Jahn-Teller active. This fact will be convenient when determining h_1' and h_1'', as h_1' only has contributions from any mode which is linearly Jahn-Teller active, where as h_1'' only has contributions from quadratically active Jahn-Teller modes.

The linear Jahn-Teller coupling constants are signed values, where as the D parameter is unsigned. The signs are not necessarily absolutely correct, a choice needs to be made to assign the phase for one mode, but the remainder are all relatively correct with respect to the first choice made. The loss of sign is due to D being related to the square of the linear coupling constant. D is a useful quantity to determine, as it is directly proportional to the stabilization energy gained via Jahn-Teller distortions. Determination of phase of the linear coupling constant, and carrying these relative phases through SOCJT 2 calculations and thus through the matrix elements of $q_{\pm}$ is done by carrying the sign of the linear coupling constant to D.

5.1.2 Derivatives of The Rotational Constant

The first derivatives of both the inertial tensor and the rotational constant for C_5H_5 are presented in Tables 5.2- 5.3. The first derivatives for all vibrational modes are presented. For second derivatives, the diagonal second derivatives–ie those which are taken with respect to a singular vibrational mode–are presented in Tables 5.4- 5.5. In total, there are $(3N-6)*(3N-6)$ total available second derivative matrices of the rotational constant as the derivatives can be taken with respect to either mode. In practice, the number can be reduced by acknowledging that only the upper diagonal is needed, as the relation

$$\frac{\partial^2 \mathbf{B}}{\partial q_i \partial q_j} = \frac{\partial^2 \mathbf{B}}{\partial q_j \partial q_i} \tag{5.1}$$

Mode Number	**Mode Symmetry**	**Reference (anion) frequency** (cm^{-1})	**Linear coupling constant**(cm^{-1})	**Quadratic coupling constant** (cm^{-1})	**K parameter**	**D parameter**
q_1	a_1'	3215.5				
q_2	a_1'	1154.9				
q_3	a_2'	1276.7				
q_4	a_2''	676.1				
q_5	e_1'	3191.1		-2.75	*-0.00086177*	
q_6	e_1'	1485.1		24.2	*0.01629519*	
q_7	e_1'	1024.5		-10.75	*-0.010492923*	
q_8	e_2'	3165.9	-42.9			*(-)8.09396E-05*
q_9	e_2'	1421	1703.5			*0.634506116*
q_{10}	e_2'	1072.7	-959.6			*(-)0.358097239*
q_{11}	e_2'	846.7	-519.2			*(-)0.184852507*
q_{12}	e_1''	643.2		72.45	*0.1577954191*	
q_{13}	e_2''	792.3				
q_{14}	e_2''	625.2				

Table 5.1: Harmonic frequencies and Linear and Quadratic Jahn-Teller coupling constants for C_5H_5. While D is the proportional to the square of the linear coupling constant and thus a positive number, the sign of the linear coupling constant is carried to the D value, indicated by leading parenthesis.

In the interests of brevity, while all possible derivatives are readily available via MATLAB calculation, only the mixed derivatives of the Jahn-Teller modes of interest, e_1' and e_2' are presented in Tables 5.6- 5.7.

More important than the derivatives in the Cartesian basis are those in the cylindrical basis. The transformation between these two coordinate system was the topic of Chapter 3. Transforming between coordinate systems is only done for the Jahn-Teller active modes of interest. These derivatives are presented in Tables 5.8- 5.10.

In order to calculate h_1' and h_1'', the most important quantities are the derivatives with respect to the cylindrical coordinates. Worth noting is where zeros are calculated. All presented zeros are calculated values, however group theoretical methods agree with calculated zero versus non-zero quantities. For example, Equation 3.26 reveals which calculated quantities of Table 5.3 should be zero and relations between the calculated nonzero values, all of which are in agreement.

It is worth noting that the first derivatives of the rotational constant for e_1' vibrational modes in the cylindrical basis are all zero, where as the second derivatives of e_2' vibrational modes in the cylindrical basis are all zero. This result implies that h_1' only can have nonzero contributions from e_2' vibrational modes, which are modes which have linear Jahn-Teller effects only. Similarly, h_1'' can only have nonzero contributions from e_1' vibrational modes, which are modes which have quadratic Jahn-Teller effects only. To a first order approximation, only the e_2' modes must be considered, and to add a second order correction to C_5H_5 , only the e_1' modes need be considered.

5.2 Vibrationless State

The vibrationless state of C_5H_5 is an excellent candidate for testing the methodology, as it has a well determined value for h_1. Yu *et. al.* fit a rotationally resolved spectra of the $\widetilde{A}^2A_2'' \leftarrow \widetilde{X}^2E_1''$ 0_0^0 laser induced fluoresence spectra, as shown in Figure 5.2.[12] From the analysis of this spectra, an experimental value for the magnitude of h_1 was determined to be 0.00706 cm^{-1}. Utilizing our methodology, as evidenced by Table 5.11, we calculate to a

Vibration	$\frac{\partial I_{xx}}{\partial q}$	$\frac{\partial I_{xy}}{\partial q}$	$\frac{\partial I_{xz}}{\partial q}$	$\frac{\partial I_{yx}}{\partial q}$	$\frac{\partial I_{yy}}{\partial q}$	$\frac{\partial I_{yz}}{\partial q}$	$\frac{\partial I_{zx}}{\partial q}$	$\frac{\partial I_{zy}}{\partial q}$	$\frac{\partial I_{zz}}{\partial q}$
q_1 (3215.495)	0.72664081	0	0	0	1.4532816	0	0	0	0.72664081
q_2 (1154.903)	-6.4079173	0	0	0	-12.815835	0	0	0	-6.4079173
q_3 (1276.724)	0	0	0	0	0	0	0	0	0
q_4 (676.113)	0	0	0	0	0	0	0	0	0
q_{5a} (3191.128)	0	0	0	0	0	0	0	0	0
q_{5b} (3191.128)	0	0	0	0	0	0	0	0	0
q_{6a} (1485.147)	0	0	0	0	0	0	0	0	0
q_{6b} (1485.147)	0	0	0	0	0	0	0	0	0
q_{7a} (1024.479)	0	0	0	0	0	0	0	0	0
q_{7b} (1024.479)	0	0	0	0	0	0	0	0	0
q_{8a} (3165.919)	-0.62879046	0	0	0	0	0	0	0	0.62879047
q_{8b} (3165.919)	0	0	-0.62879046	0	0	0	-0.62879046	0	0
q_{9a} (1420.997)	-1.2148628	0	0	0	0	0	0	0	1.2148628
q_{9b} (1420.997)	0	0	1.2148628	0	0	0	1.2148628	0	0
q_{10a} (1072.714)	-4.773736	0	0	0	0	0	0	0	4.773736
q_{10b} (1072.714)	0	0	4.773736	0	0	0	4.773736	0	0
q_{11a} (846.683)	5.0186365	0	0	0	0	0	0	0	-5.0186365
q_{11b} (846.683)	0	0	5.0186365	0	0	0	5.0186365	0	0
q_{12a} (643.154)	0	0	0	0	0	3.413059e-05	0	3.413059e-05	0
q_{12b} (643.154)	0	3.4127811e-05	0	3.4127811e-05	0	0	0	0	0
q_{13a} (792.333)	0	0	0	0	0	0	0	0	0
q_{13b} (792.333)	0	0	0	0	0	0	0	0	0
q_{14a} (625.186)	0	0	0	0	0	0	0	0	0
q_{14b} (625.186)	0	0	0	0	0	0	0	0	0

Table 5.2: First derivatives of Inertial tensor calculated using third order finite differentiation with stepsize of 1e-05. Units are amu^{1}bohr^2. The molecule lies in the xz plane.

Vibration	$\frac{\partial B_{xx}}{\partial q}$	$\frac{\partial B_{xy}}{\partial q}$	$\frac{\partial B_{xz}}{\partial q}$	$\frac{\partial B_{yx}}{\partial q}$	$\frac{\partial B_{yy}}{\partial q}$	$\frac{\partial B_{yz}}{\partial q}$	$\frac{\partial B_{zx}}{\partial q}$	$\frac{\partial B_{zy}}{\partial q}$	$\frac{\partial B_{zz}}{\partial q}$
q_1 (3215.495)	-0.00105126	0	0	0	-0.00052562998	0	0	0	-0.00105126
q_2 (1154.903)	0.0092705872	0	0	0	0.0046352936	0	0	0	0.0092705872
q_3 (1276.724)	0	0	0	0	0	0	0	0	0
q_4 (676.113)	0	0	0	0	0	0	0	0	0
q_{5a} (3191.128)	0	0	0	0	0	0	0	0	0
q_{5b} (3191.128)	0	0	0	0	0	0	0	0	0
q_{6a} (1485.147)	0	0	0	0	0	0	0	0	0
q_{6b} (1485.147)	0	0	0	0	0	0	0	0	0
q_{7a} (1024.479)	0	0	0	0	0	0	0	0	0
q_{7b} (1024.479)	0	0	0	0	0	0	0	0	0
q_{8a} (3165.919)	0.000909696	0	0	0	0	0	0	0	-0.00090969601
q_{8b} (3165.919)	0	0	0.000909696	0	0	0	0.000909696	0	0
q_{9a} (1420.997)	0.00175759	0	0	0	0	0	0	0	-0.0017575901
q_{9b} (1420.997)	0	0	-0.0017575901	0	0	0	-0.0017575901	0	0
q_{10a} (1072.714)	0.0069063525	0	0	0	0	0	0	0	-0.0069063525
q_{10b} (1072.714)	0	0	-0.0069063525	0	0	0	-0.0069063525	0	0
q_{11a} (846.683)	-0.0072606597	0	0	0	0	0	0	0	0.0072606597
q_{11b} (846.683)	0	0	-0.0072606597	0	0	0	-0.0072606597	0	0
q_{12a} (643.154)	0	0	0	0	0	-2.4689036e-08	0	-2.4689036e-08	0
q_{12b} (643.154)	0	-2.4687026e-08	0	-2.4687026e-08	0	0	0	0	0
q_{13a} (792.333)	0	0	0	0	0	0	0	0	0
q_{13b} (792.333)	0	0	0	0	0	0	0	0	0
q_{14a} (625.186)	0	0	0	0	0	0	0	0	0
q_{14b} (625.186)	0	0	0	0	0	0	0	0	0

Table 5.3: Derivatives of rotational constant of C_5H_5 calculated utilizing the relations of Equation 3.11 and the derivatives of the inertial tensor from Table 5.2. Units are wavenumber. The molecule lies in the xz plane.

Vibration	$\frac{\partial^2 I_{xx}}{\partial q_i \partial q_j}$	$\frac{\partial^2 I_{xy}}{\partial q_i \partial q_j}$	$\frac{\partial^2 I_{xz}}{\partial q_i \partial q_j}$	$\frac{\partial^2 I_{yx}}{\partial q_i \partial q_j}$	$\frac{\partial^2 I_{yy}}{\partial q_i \partial q_j}$	$\frac{\partial^2 I_{yz}}{\partial q_i \partial q_j}$	$\frac{\partial^2 I_{zx}}{\partial q_i \partial q_j}$	$\frac{\partial^2 I_{zy}}{\partial q_i \partial q_j}$	$\frac{\partial^2 I_{zz}}{\partial q_i \partial q_j}$
q_1 (3215.495)	0.038653525	0	0	0	0.079580786	0	0	0	0.036379788
q_2 (1154.903)	0.10345502	0	0	0	0.21145752	0	0	0	0.10345502
q_3 (1276.724)	0.094360075	0	-6.1679057e-06	0	0.19326762	0	-6.1679057e-06	0	0.094360075
q_4 (676.113)	0.3558398	0	0	0	0.0022737368	0	0	0	0.35356607
q_{5a} (3191.128)	0.056843419	0	0	0	0.079580786	0	0	0	0.019326762
q_{5b} (3191.128)	0.019326762	0	-1.6283271e-06	0	0.079580786	0	-1.6283271e-06	0	0.05570655
q_{6a} (1485.147)	0.10345502	0	0	0	0.16598278	0	0	0	0.059117156
q_{6b} (1485.147)	0.057980287	0	5.2797273e-05	0	0.16598278	0	5.2797273e-05	0	0.10118129
q_{7a} (1024.479)	0.14551915	0	0	0	0.23874236	0	0	0	0.088675733
q_{7b} (1024.479)	0.089812602	0	-4.9343246e-06	0	0.23874236	0	-4.9343246e-06	0	0.14551915
q_{8a} (3165.919)	0.037516656	0	0	0	0.079580786	0	0	0	0.036379788
q_{8b} (3165.919)	0.038653525	0	0	0	0.079580786	0	0	0	0.036379788
q_{9a} (1420.997)	0.085265128	0	0	0	0.17507773	0	0	0	0.082991392
q_{9b} (1420.997)	0.08412826	0	4.7961648e-05	0	0.17053026	0	4.7961648e-05	0	0.08412826
q_{10a} (1072.714)	0.1114131	0	0	0	0.22737368	0	0	0	0.1114131
q_{10b} (1072.714)	0.11254997	0	0	0	0.22737368	0	0	0	0.11254997
q_{11a} (846.683)	0.14210855	0	0	0	0.28876457	0	0	0	0.14210855
q_{11b} (846.683)	0.14210855	0	-3.9968029e-05	0	0.28649083	0	-3.9968029e-05	0	0.13983481
q_{12a} (643.154)	0.37289283	0	0	0	0.0022737368	0	0	0	0.3740297
q_{12b} (643.154)	0.3740297	0	0	0	0.0022737368	0	0	0	0.37175596
q_{13a} (792.333)	0.30468073	0	0	0	0.0022737368	0	0	0	0.30354386
q_{13b} (792.333)	0.30581759	0	0	0	0.0022737368	0	0	0	0.30354386
q_{14a} (625.186)	0.38539838	0	0	0	0.0022737368	0	0	0	0.38539838
q_{14a} (625.186)	0.38426151	0	0	0	0.0022737368	0	0	0	0.38426151

Table 5.4: Diagonal second derivatives of inertial tensor for C_5H_5 calculated using third order finite differentiation with stepsize of 5e-05. Units are amu[1]bohr[2]. These derivatives are taken with respect to a singular vibration, $q_i = q_j$.

Vibration	$\frac{\partial^2 B_{xx}}{\partial q_i \partial q_j}$	$\frac{\partial^2 B_{xz}}{\partial q_i \partial q_j}$	$\frac{\partial^2 B_{xy}}{\partial q_i \partial q_j}$	$\frac{\partial^2 B_{yx}}{\partial q_i \partial q_j}$	$\frac{\partial^2 B_{yy}}{\partial q_i \partial q_j}$	$\frac{\partial^2 B_{yz}}{\partial q_i \partial q_j}$	$\frac{\partial^2 B_{zx}}{\partial q_i \partial q_j}$	$\frac{\partial^2 B_{zy}}{\partial q_i \partial q_j}$	$\frac{\partial^2 B_{zz}}{\partial q_i \partial q_j}$
q_1	-0.0000466801	0	0	0	-0.0000233400	0	0	0	-0.0000466800
q_2	0.0004315934	0	0	0	0.0002157969	0	0	0	0.0004315935
q_3	-0.0001364358	0	0	0	-0.0000682177	0	0	0	-0.0001364355
q_4	-0.0005152796	0	-0	0	0	-0	-0	-0	-0.0005152796
q_{5a}	-0.0000810077	0	0	0	-0.0000272934	0	0	0	-0.0000281661
q_{5b}	-0.0000281662	0	0	0	-0.0000272933	0	0	0	-0.0000810074
q_{6a}	-0.0001493083	0	0	0	-0.0000586411	0	0	0	-0.0000852567
q_{6b}	-0.0000852568	0	0	0	-0.0000586412	0	0	0	-0.0001493082
q_{7a}	-0.0002113349	0	0	0	-0.0000850134	0	0	0	-0.0001287191
q_{7b}	-0.0001287192	0	0	0	-0.0000850134	0	0	0	-0.0002113348
q_{8a}	-0.0000494113	0	0	0	-0.0000275107	0	0	0	-0.0000494112
q_{8b}	-0.0000494112	0	0	0	-0.0000275107	0	0	0	-0.0000494111
q_{9a}	-0.0001016445	0	0	0	-0.0000612871	0	0	0	-0.0001016444
q_{9b}	-0.0001016445	0	0	0	-0.0000612870	0	0	0	-0.0001016443
q_{10a}	0.0001608685	0	0	0	-0.0000811918	0	0	0	0.0001608687
q_{10b}	0.0001608685	0	0	0	-0.0000811917	0	0	0	0.0001608686
q_{11a}	0.0001515096	0	0	0	-0.0001028594	0	0	0	0.0001515098
q_{11b}	0.0001515096	0	0	0	-0.0001028594	0	0	0	0.0001515097
q_{12a}	-0.0005416759	0	0	0	0	0	0	0	-0.0005416759
q_{12b}	-0.0005416760	0	0	0	0	0	0	0	-0.0005416760
q_{13a}	-0.0004396976	0	0	0	0	0	0	0	-0.0004396975
q_{13b}	-0.0004396976	0	-0	0	0	0	-0	0	-0.0004396975
q_{14a}	-0.0005572013	0	0	0	0	-0	0	-0	-0.0005572014
q_{14b}	-0.0005572012	-0	-0	-0	0	0	-0	0	-0.0005572012

Table 5.5: Diagonal second derivatives of the rotational constant for C_5H_5 calculated utilizing Equation 3.15 and the values from Table 5.2 and Table 5.4. Units are wavenumber. These derivatives are taken with with respect to a singular vibration, $q_i = q_j$.

q_i	q_j	$\frac{\partial^2 B_{xx}}{\partial q_i \partial q_j}$	$\frac{\partial^2 B_{xz}}{\partial q_i \partial q_j}$	$\frac{\partial^2 B_{xy}}{\partial q_i \partial q_j}$	$\frac{\partial^2 B_{yx}}{\partial q_i \partial q_j}$	$\frac{\partial^2 B_{yy}}{\partial q_i \partial q_j}$	$\frac{\partial^2 B_{yz}}{\partial q_i \partial q_j}$	$\frac{\partial^2 B_{zx}}{\partial q_i \partial q_j}$	$\frac{\partial^2 B_{zy}}{\partial q_i \partial q_j}$	$\frac{\partial^2 B_{zz}}{\partial q_i \partial q_j}$
q_{8a}	q_{8a}	-0.0000494113	0	0	0	-0.0000275107	0	0	0	-0.0000494112
q_{8a}	q_{8b}	-0	0	0	0	-0	0	0	0	-0
q_{8a}	q_{9a}	0.0000108371	0	0	0	0	0	0	0	0.0000108372
q_{8a}	q_{9b}	0	0	0	0	-0	0	0	0	0
q_{8a}	q_{10a}	0.0000425855	0	0	0	0	0	0	0	0.0000425856
q_{8a}	q_{10b}	0	0	-0	0	-0	0	-0	0	0
q_{8a}	q_{11a}	-0.0000447654	0	0	0	0	0	0	0	-0.0000447653
q_{8a}	q_{11b}	0	0	-0	0	0	0	-0	0	0
q_{8b}	q_{8b}	-0.0000494112	0	0	0	-0.0000275107	0	0	0	-0.0000494111
q_{8b}	q_{9a}	-0	0	0	0	-0	0	0	0	-0
q_{8b}	q_{9b}	0.0000108371	0	-0	0	0	0	-0	0	0.0000108371
q_{8b}	q_{10a}	0	0	-0	0	-0	0	-0	0	-0
q_{8b}	q_{10b}	0.0000425855	0	0	0	0	0	0	0	0.0000425855
q_{8b}	q_{11a}	0	0	-0	0	0	0	-0	0	0
q_{8b}	q_{11b}	-0.0000447654	0	0	0	0	0	0	0	-0.0000447654
q_{9a}	q_{9a}	-0.0001016445	0	0	0	-0.0000612871	0	0	0	-0.0001016444
q_{9a}	q_{9b}	-0	0	0	0	-0	0	0	0	0
q_{9a}	q_{10a}	0.0000822582	0	0	0	0	0	0	0	0.0000822580
q_{9a}	q_{10b}	0	0	0	0	-0	0	0	0	-0
q_{9a}	q_{11a}	-0.0000864667	0	0	0	0	0	0	0	-0.0000864667
q_{9a}	q_{11b}	-0	0	-0	0	0	0	-0	0	-0
q_{9b}	q_{9b}	-0.0001016445	0	0	0	-0.0000612870	0	0	0	-0.0001016443
q_{9b}	q_{10a}	0	0	-0	0	0	0	-0	0	0
q_{9b}	q_{10b}	0.0000822580	0	0	0	0	0	0	0	0.0000822580
q_{9b}	q_{11a}	-0	0	-0	0	0	0	-0	0	0
q_{9b}	q_{11b}	-0.0000864668	0	-0	0	0	0	-0	0	-0.0000864667
q_{10a}	q_{10a}	0.0001608685	0	0	0	-0.0000811918	0	0	0	0.0001608687
q_{10a}	q_{10b}	0	0	-0	0	-0	0	-0	0	-0
q_{10a}	q_{11a}	-0.0003398219	0	0	0	0	0	0	0	-0.0003398219
q_{10a}	q_{11b}	-0	0	-0	0	0	0	-0	0	-0
q_{10b}	q_{10b}	0.0001608685	0	0	0	-0.0000811917	0	0	0	0.0001608686
q_{10b}	q_{11a}	-0	0	-0	0	-0	0	-0	0	-0
q_{10b}	q_{11b}	-0.0003398220	0	0	0	0	0	0	0	-0.0003398220
q_{11a}	q_{11a}	0.0001515096	0	0	0	-0.0001028594	0	0	0	0.0001515098
q_{11a}	q_{11b}	0	0	0	0	-0	0	0	0	-0
q_{11b}	q_{11b}	0.0001515096	0	0	0	-0.0001028594	0	0	0	0.0001515097

Table 5.6: Mixed second derivatives of the rotational constant for e_2' vibrations of C_5H_5 calculated utilizing Equation 3.15 and the values from Table 5.2 and Table 5.4. Units are wavenumber.

q_i	q_j	$\frac{\partial^2 B_{xx}}{\partial q_i \partial q_j}$	$\frac{\partial^2 B_{xz}}{\partial q_i \partial q_j}$	$\frac{\partial^2 B_{xy}}{\partial q_i \partial q_j}$	$\frac{\partial^2 B_{yx}}{\partial q_i \partial q_j}$	$\frac{\partial^2 B_{yy}}{\partial q_i \partial q_j}$	$\frac{\partial^2 B_{yz}}{\partial q_i \partial q_j}$	$\frac{\partial^2 B_{zx}}{\partial q_i \partial q_j}$	$\frac{\partial^2 B_{zy}}{\partial q_i \partial q_j}$	$\frac{\partial^2 B_{zz}}{\partial q_i \partial q_j}$
q_{5a}	q_{5a}	-0.0000810077	0	0	0	-0.0000272934	0	0	0	-0.0000281661
q_{5a}	q_{5b}	0	0	-0.0000264207	0	0	0	-0.0000264207	0	0
q_{5a}	q_{6a}	-0.0000290900	0	0	0	0	0	0	0	0.0000290871
q_{5a}	q_{6b}	-0	0	-0.0000290885	0	-0	0	-0.0000290885	0	0
q_{5a}	q_{7a}	0.0000330344	0	0	0	0	0	0	0	-0.0000330377
q_{5a}	q_{7b}	0	0	0.0000330361	0	0	0	0.0000330361	0	-0
q_{5b}	q_{5b}	-0.0000281662	0	0	0	-0.0000272933	0	0	0	-0.0000810074
q_{5b}	q_{6a}	-0	0	-0.0000290885	0	0	0	-0.0000290885	0	-0
q_{5b}	q_{6b}	0.0000290872	0	-0	0	0	0	-0	0	-0.0000290900
q_{5b}	q_{7a}	0	0	0.0000330360	0	0	0	0.0000330360	0	-0
q_{5b}	q_{7b}	-0.0000330376	0	-0	0	0	0	-0	0	0.0000330344
q_{6a}	q_{6a}	-0.0001493083	0	0	0	-0.0000586411	0	0	0	-0.0000852567
q_{6a}	q_{6b}	0	0	-0.0000320257	0	-0	0	-0.0000320257	0	-0
q_{6a}	q_{7a}	0.0000363787	0	0	0	0	0	0	0	-0.0000363652
q_{6a}	q_{7b}	0	0	0.0000363719	0	0	0	0.0000363719	0	-0
q_{6b}	q_{6b}	-0.0000852568	0	0	0	-0.0000586412	0	0	0	-0.0001493082
q_{6b}	q_{7a}	-0	0	0.0000363719	0	-0	0	0.0000363719	0	-0
q_{6b}	q_{7b}	-0.0000363652	0	0	0	0	0	0	0	0.0000363787
q_{7a}	q_{7a}	-0.0002113349	0	0	0	-0.0000850134	0	0	0	-0.0001287191
q_{7a}	q_{7b}	0	0	-0.0000413078	0	0	0	-0.0000413078	0	0
q_{7b}	q_{7b}	-0.0001287192	0	0	0	-0.0000850134	0	0	0	-0.0002113348

Table 5.7: Mixed second derivatives of the rotational constant for e_1' vibrations of C_5H_5 calculated utilizing Equation 3.15 and the values from Table 5.2 and Table 5.4. Units are wavenumber.

q_{i,r_i}	$\frac{\partial B_{++}}{\partial q_{i,r_i}}$	$\frac{\partial B_{--}}{\partial q_{i,r_i}}$
q_{5+}	0	0
q_{5-}	0	0
q_{6+}	0	0
q_{6-}	0	0
q_{7+}	0	0
q_{7-}	0	0
q_{8+}	0	0.00049848
q_{8-}	0.00049848	0
q_{9+}	0	0.000878795
q_{9-}	0.000878795	0
q_{10+}	0	0.0034531765
q_{10-}	0.0034531765	0
q_{11+}	0	-0.00363033
q_{11-}	-0.00363033	0

Table 5.8: First derivatives of the rotational constant for C_5H_5 with respect to Jahn-Teller active vibrational modes represented in cylindrical coordinates. Units are wavenumber.

first order approximation the magnitude of h_1 to be 0.00691 cm^{-1}.

To a first order approximation, this is excellent agreement between experimental and theoretical results. While in Table 5.11 there is a sign discrepancy between the experimental value and the calculated value, this can be accounted for in one of two ways. First, experimentally, it is not possible to determine a sign for h_1, rather only a magnitude. Alternatively, derivatives and matrix elements are based upon an electronic structure calculation which makes a choice for phase and keeps all other choices relatively consistent. The opposite choice could be made for the direction to take the first derivative, at which point all subsequent quantities would remain relatively consistent, but with a sign change, in this sense only a magnitude of h_1' is available.

5.3 Vibrationally Excited States

The ground state was useful for testing the methodology, but the extension to vibrationally excited states provides the possibility to apply this method to numerous experimental spectra. Recently, Leicht et. al. took an IR spectra of the cyclopentadienyl radical solvated in

q_{i,r_i}	q_{j,r_j}	$\frac{\partial B_{++}}{\partial q_{i,r_i}} q_{j,r_j}$	$\frac{\partial B_{--}}{\partial q_{i,r_i}} q_{j,r_j}$
q_{5+}	q_{5+}	0	0.0000132104
q_{5+}	q_{5-}	0	0
q_{5-}	q_{5+}	0	0
q_{5-}	q_{5-}	0.0000132104	0
q_{5+}	q_{6+}	0	0.0000145444
q_{5+}	q_{6-}	0	0
q_{5-}	q_{6+}	0	0
q_{5-}	q_{6-}	0.0000145444	0
q_{5+}	q_{7+}	0	-0.0000165180
q_{5+}	q_{7-}	0	0
q_{5-}	q_{7+}	0	0
q_{5-}	q_{7-}	-0.0000165180	0
q_{6+}	q_{5+}	0	0.0000145444
q_{6+}	q_{5-}	0	0
q_{6-}	q_{5+}	0	0
q_{6-}	q_{5-}	0.0000145444	0
q_{6+}	q_{6+}	0	0.0000160131
q_{6+}	q_{6-}	0	0
q_{6-}	q_{6+}	0	0
q_{6-}	q_{6-}	0.0000160131	0
q_{6+}	q_{7+}	0	-0.0000181860
q_{6+}	q_{7-}	0	0
q_{6-}	q_{7+}	0	0
q_{6-}	q_{7-}	-0.0000181860	0
q_{7+}	q_{5+}	0	-0.0000165180
q_{7+}	q_{5-}	0	0
q_{7-}	q_{5+}	0	0
q_{7-}	q_{5-}	-0.0000165180	0
q_{7+}	q_{6+}	0	-0.0000181860
q_{7+}	q_{6-}	0	0
q_{7-}	q_{6+}	0	0
q_{7-}	q_{6-}	-0.0000181860	0
q_{7+}	q_{7+}	0	0.0000206532
q_{7+}	q_{7-}	0	0
q_{7-}	q_{7+}	0	0
q_{7-}	q_{7-}	0.0000206532	0

Table 5.9: Second derivatives of the rotational constant for e_1' vibrational modes of C_5H_5 in cylindrical coordinates. Units are wavenumber.

q_{i,r_i}	q_{j,r_j}	$\frac{\partial^2 B_{++}}{\partial q_{i,r_i}\partial q_{j,r_j}}$	$\frac{\partial^2 B_{--}}{\partial q_{i,r_i}\partial q_{j,r_j}}$	q_{i,r_i}	q_{j,r_j}	$\frac{\partial^2 B_{++}}{\partial q_{i,r_i}\partial q_{j,r_j}}$	$\frac{\partial^2 B_{--}}{\partial q_{i,r_i}\partial q_{j,r_j}}$
q_{8+}	q_{8+}	0	0	q_{10+}	q_{8+}	0	0
q_{8+}	q_{8-}	0	0	q_{10+}	q_{8-}	0	0
q_{8-}	q_{8+}	0	0	q_{10-}	q_{8+}	0	0
q_{8-}	q_{8-}	0	0	q_{10-}	q_{8-}	0	0
q_{8+}	q_{9+}	0	0	q_{10+}	q_{9+}	0	0
q_{8+}	q_{9+}	0	0	q_{10+}	q_{9-}	0	0
q_{8+}	q_{9+}	0	0	q_{10-}	q_{9+}	0	0
q_{8+}	q_{9+}	0	0	q_{10-}	q_{9-}	0	0
q_{8+}	q_{10+}	0	0	q_{10+}	q_{10+}	0	0
q_{8+}	q_{10+}	0	0	q_{10+}	q_{10-}	0	0
q_{8+}	q_{10+}	0	0	q_{10-}	q_{10+}	0	0
q_{8+}	q_{10+}	0	0	q_{10-}	q_{10-}	0	0
q_{8+}	q_{11+}	0	0	q_{10+}	q_{11+}	0	0
q_{8+}	q_{11-}	0	0	q_{10+}	q_{11-}	0	0
q_{8-}	q_{11+}	0	0	q_{10-}	q_{11+}	0	0
q_{8-}	q_{11-}	0	0	q_{10-}	q_{11-}	0	0
q_{9+}	q_{8+}	0	0	q_{11+}	q_{8+}	0	0
q_{9+}	q_{8-}	0	0	q_{11+}	q_{8-}	0	0
q_{9-}	q_{8+}	0	0	q_{11-}	q_{8+}	0	0
q_{9-}	q_{8-}	0	0	q_{11-}	q_{8-}	0	0
q_{9+}	q_{9+}	0	0	q_{11+}	q_{9+}	0	0
q_{9+}	q_{9-}	0	0	q_{11+}	q_{9-}	0	0
q_{9-}	q_{9+}	0	0	q_{11-}	q_{9+}	0	0
q_{9-}	q_{9-}	0	0	q_{11-}	q_{9-}	0	0
q_{9+}	q_{10+}	0	0	q_{11+}	q_{10+}	0	0
q_{9+}	q_{10-}	0	0	q_{11+}	q_{10-}	0	0
q_{9-}	q_{10+}	0	0	q_{11-}	q_{10+}	0	0
q_{9-}	q_{10-}	0	0	q_{11-}	q_{10-}	0	0
q_{9+}	q_{11+}	0	0	q_{11+}	q_{11+}	0	0
q_{9+}	q_{11-}	0	0	q_{11+}	q_{11-}	0	0
q_{9-}	q_{11+}	0	0	q_{11-}	q_{11+}	0	0
q_{9-}	q_{11-}	0	0	q_{11-}	q_{11-}	0	0

Table 5.10: Second derivatives of the rotational constant for e_2' vibrational modes of C_5H_5 in cylindrical coordinates. Symmetry dictates all values should be zero, as is calculated numerically. Units are wavenumber.

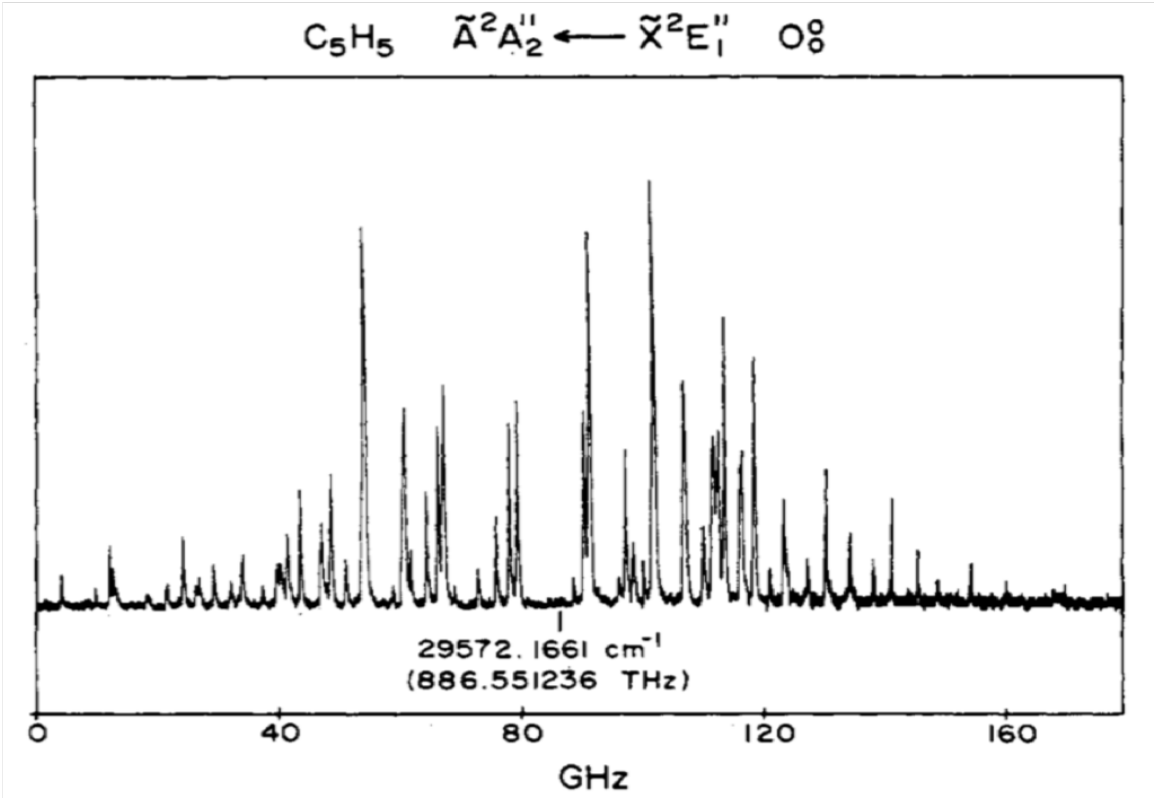

Figure 5.2: Rotationally resolved electronic spectra of cyclopentadienyl radical available in Reference [12]

Vibrational Mode	$\frac{\partial \mathbf{B}_{\pm\pm}}{\partial q_{\mp}}$	$\langle E'_{2+}\vert\, q_{\pm}\,\vert E'_{2-}\rangle + \langle E'_{2-}\vert\, q_{\mp}\,\vert E'_{2+}\rangle$
q_8	-0.00363	1.331572
q_9	0.00345	-1.94297
q_{10}	0.000879	-2.60409
q_{11}	0.000498	0.024777
Predicted h_1	-0.00691	
Experimental Magnitude h_1	0.00706	

Table 5.11: h'_1 value predicted for the vibrationless state of the cyclopentadienyl radical. Derivatives of the rotational constant and values for h_1 have units of wavenumber, while the matrix elements are dimensionless.

helium nanodroplets in the C-H stretch region. As seen in Figure 5.3, the Jahn-Teller splitting of a vibrational band is approximately 30 cm^{-1}. However, theoretical methods predict this splitting to only be about 3cm^{-1}. Are theoretical methods inaccurate? Or are the transitions improperly assigned? Figure 5.4 represents potentially Jahn-Teller active levels in the C-H stretch region. Clearly, there are many possible levels in this range that could be bright in an experimental spectra. The optimal way to assign the transitions in this region is to collect rotationally resolved vibrational spectra. With this spectra, predicted h_1 values can be used to simulate the rotational structure to match proper state assignments, or the spectra can be fit to a Jahn-Teller Hamiltonian including h_1 to match to predicted values. Current experimental work is under way toward collecting this spectra.[24]

5.3.1 Higher Order Terms

The calculation of h'_1 and h''_1 for a number of vibrationally excited states has been done and the results are present in Tables 5.12- 5.14. For the vibrationless state, the second order correction to h_1 is multiple orders of magnitude smaller than the first order correction. This is expected, as cyclopentadienyl radical has a weak Jahn-Teller effect, making the first order approximation to h_1 a good approximation. In general, values for h''_1 are up to a few orders of magnitude smaller than typical values for h'_1.

Eigenenergy	j	Vibronic Symmetry	h_1'	h_1''
0	0.5	E_{1+}''	-0.00691621	0
458.5398	1.5	E_{2+}''	0	0
869.7438	0.5	E_{1+}''	-0.00082152	0
901.6243	1.5	E_{2+}''	0	0
1041.195	2.5	E_{2-}''	0	0
1123.418	0.5	E_{1+}''	-0.00226418	0
1207.981	1.5	E_{2+}''	0	0
1313.786	0.5	E_{1+}''	0.00027156	0
1376.303	2.5	E_{2-}''	0	0
1478.653	0.5	E_{1+}''	-0.00178250	0
1683.726	3.5	E_{1-}''	0	0
1686.571	2.5	E_{2-}''	0	0
1722.162	0.5	E_{1+}''	-0.00405682	0
1735.573	1.5	E_{2+}''	0	0
1774.456	0.5	E_{1+}''	-0.00597144	0
1803.72	2.5	E_{2-}''	0	0
1856.75	1.5	E_{2+}''	0	0
1971.97	3.5	E_{1-}''	0	0
1991.372	1.5	E_{2+}''	0	0
2010.986	0.5	E_{1+}''	-0.00133490	0
2070.669	1.5	E_{2+}''	0	0
2073.837	0.5	E_{1+}''	0.00167421	0
2110.087	2.5	E_{2-}''	0	0
2179.225	0.5	E_{1+}''	-0.00115615	0
2215.566	1.5	E_{2+}''	0	0
2281.219	3.5	E_{1-}''	0	0
2281.625	1.5	E_{2+}''	0	0
2292.521	0.5	E_{1+}''	-0.00350652	0
2296.009	3.5	E_{1-}''	0	0
2329.368	1.5	E_{2+}''	0	0
2386.56	0.5	E_{1+}''	-0.00202271	0
2403.511	1.5	E_{2+}''	0	0
2413.583	2.5	E_{2-}''	0	0
2502.687	2.5	E_{2-}''	0	0
2548.842	1.5	E_{2+}''	0	0
2550.527	0.5	E_{1+}''	-0.00179942	0
2605.393	3.5	E_{1-}''	0	0
2606.911	2.5	E_{2-}''	0	0

Table 5.12: Calculated h_1' and h_1'' for vibronic states of e_2' modes

Eigenenergy	j	Vibronic Symmetry	h_1'	h_1''
2607.294	0.5	E_{1+}''	-0.00144098	0
2631.894	0.5	E_{1+}''	-0.00190943	0
2634.92	1.5	E_{2+}''	0	0
2681.675	1.5	E_{2+}''	0	0
2684.067	2.5	E_{2-}''	0	0
2703.817	0.5	E_{1+}''	0.00036291	0
2706.367	3.5	E_{1-}''	0	0
2731.829	1.5	E_{2+}''	0	0
2789.693	2.5	E_{2-}''	0	0
2851.003	0.5	E_{1+}''	-0.00081934	0
2892.418	1.5	E_{2+}''	0	0
2892.773	0.5	E_{1+}''	-0.00192312	0
2893.215	2.5	E_{2-}''	0	0
2914.618	3.5	E_{1-}''	0	0
2934.263	0.5	E_{1+}''	0.00001811	0
2956.233	1.5	E_{2+}''	0	0
2956.907	0.5	E_{1+}''	-0.00026202	0
2968.951	2.5	E_{2-}''	0	0
2984.582	1.5	E_{2+}''	0	0
2998.609	2.5	E_{2-}''	0	0
3012.621	3.5	E_{1-}''	0	0
3046.962	0.5	E_{1+}''	0.00010671	0
3055.816	1.5	E_{2+}''	0	0
3074.792	0.5	E_{1+}''	0.00009535	0
3075.519	2.5	E_{2-}''	0	0
3133.742	2.5	E_{2-}''	0	0
3142.928	0.5	E_{1+}''	-0.00127247	0
3161.611	1.5	E_{2+}''	0	0
3165.826	0.5	E_{1+}''	-0.00000021	0
3165.831	1.5	E_{2+}''	0	0
3182.812	3.5	E_{1-}''	0	0
3183.175	0.5	E_{1+}''	-0.00139951	0
3191.727	2.5	E_{2-}''	0	0
3211.645	0.5	E_{1+}''	-0.00014721	0
3251.386	2.5	E_{2-}''	0	0
3267.074	1.5	E_{2+}''	0	0
3290.069	1.5	E_{2+}''	0	0
3291.131	2.5	E_{2-}''	0	0
3295.366	0.5	E_{1+}''	-0.00254718	0

Table 5.13: Calculated h_1' and h_1'' for vibronic states of e_2' modes

Eigenenergy	Vibronic Symmetry	h_1'	h_1''
0	E_1''	0	-1.04558E-07
1013.75	A_1''	0	0
1024.444	E_2''	0	0
1035.25	A_2''	0	0
1460.9	A_2''	0	0
1484.903	E_2''	0	0
1509.301	A_1''	0	0
2033.783	E_1''	0	1.87695E-05
2048.859	E_2''	0	0
2064.188	E_1''	0	-1.85968E-05
2483.08	E_1''	0	-5.44798E-06
2509.346	E_2''	0	0
2509.426	E_1''	0	-2.47306E-07
2536.04	E_1''	0	5.69528E-06
2935.926	E_1''	0	-2.29622E-05
2969.707	E_2''	0	0
3004.375	E_1''	0	2.23357E-05
3051.972	A_1''	0	0
3054.853	E_2''	0	0
3073.246	E_1''	0	0
3092.091	E_1''	0	0
3094.971	A_2''	0	0
3188.35	A_1''	0	0
3191.099	E_2''	0	0
3193.85	A_2''	0	0
3502.493	A_2''	0	0
3505.449	E_2''	0	0

Table 5.14: Calculated h_1' and h_1'' for vibronic states of e_1' modes

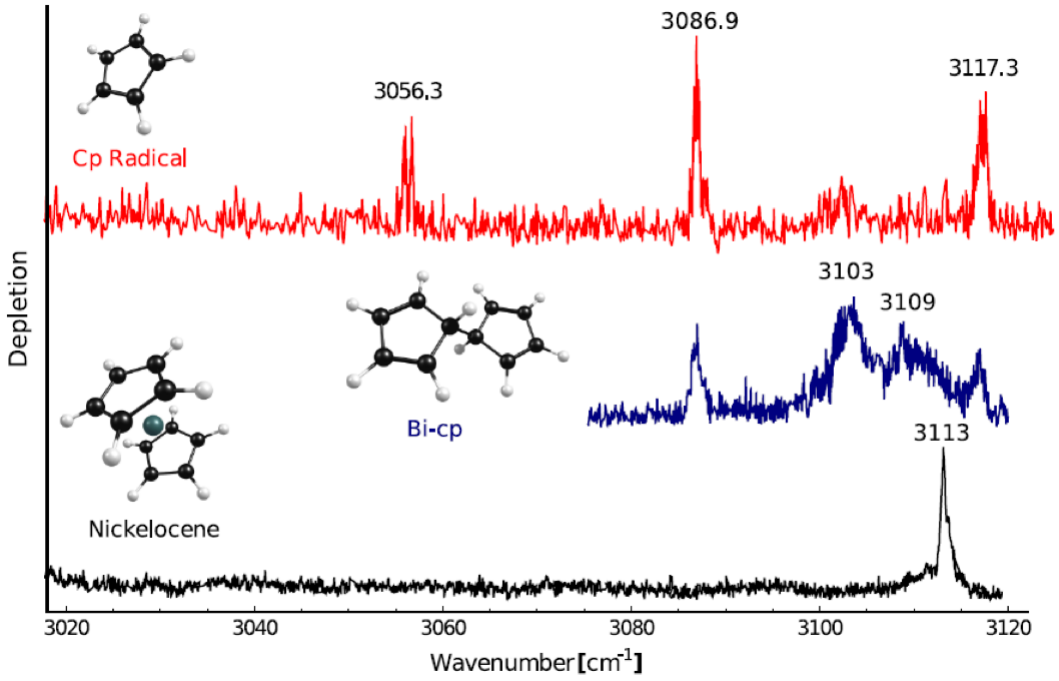

Figure 5.3: IR Spectrum recorded by Reference .[23] The claimed Jahn-Teller splitting of the q_5 fundamental is approximately 30 cm^{-1}, which is an order of magnitude larger splitting than theoretical methods would predict.

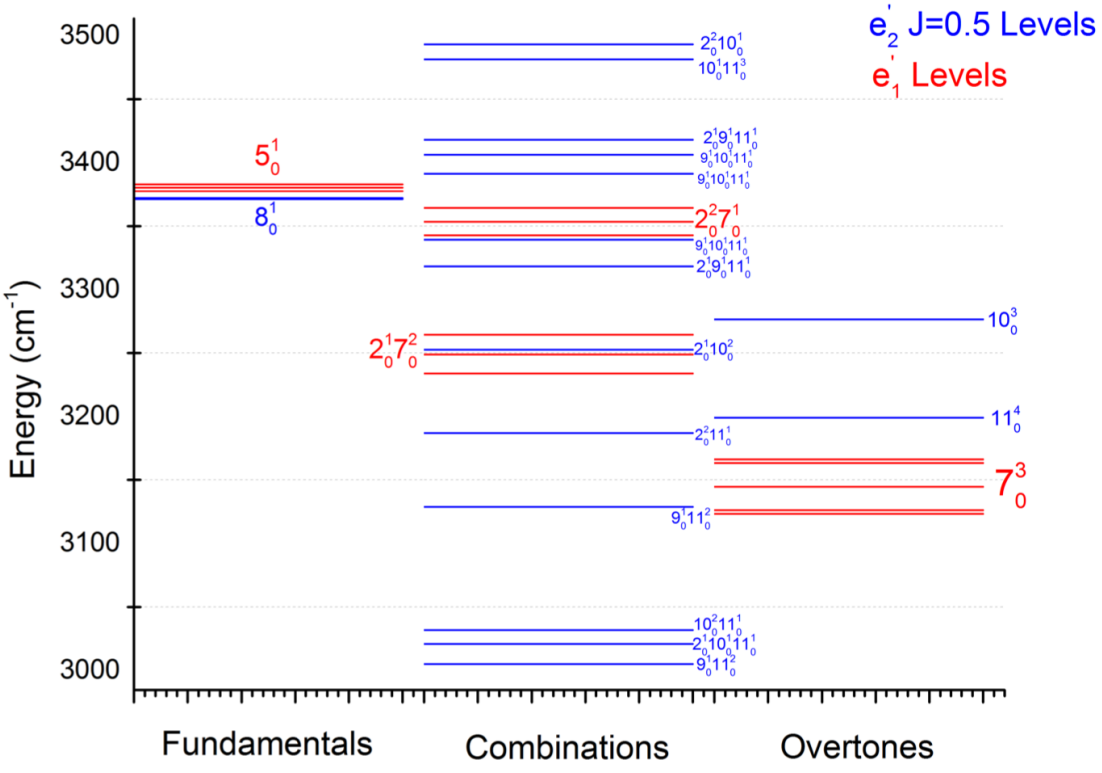

Figure 5.4: Possible vibrational transitions in the C-H stretch region using electronic structure harmonic frequencies and Jahn-Teller couplings. Inclusion on anharmonic terms could potentially lower the levels to the proper vibrational energies as seen in the experimental spectra. This diagram includes no comments on the intensity of transitions to these levels, only their existence.

Chapter 6
Nitrate Results

6.1 The Molecule

The nitrate radical has remained a highly contentious molecule between theory and experiment.[25,26,27,28] Experimental data suggests small geometric distortions, while theory would predict very large Jahn-Teller distortions.[29,30] Group theoretically, it would at first appear that NO_3 would be an easier problem to solved than the C_5H_5 , as there are 6 fewer atoms and lower total symmetry. However, because the Jahn-Teller effect is stronger in NO_3, the vibrational modes feature linear, quadratical and higher orders of Jahn-Teller activity, along with coupling between the degenerate vibrations, NO_3 is arguably a much more complex molecule.

In NO_3 the $\widetilde{A}^2E''$ is Jahn-Teller active. Experimentally, both vibrationally and rotationally resolved spectra of the $\widetilde{A}^2E'' \leftarrow \widetilde{X}^2A_2'$ electronic transition have been recorded.[13] Theoretical calculations have also been performed for both the $\widetilde{X}^2A_2'$ and $\widetilde{A}^2E''$.[25,26,27] Experimentally, an upper bound has been determined for the magnitude of h_1.[31] Our methodology for determining h_1 for NO_3 parallels the calculation for C_5H_5.

6.1.1 Derivatives of The Rotational Constant

The first derivatives of the inertial tensor and rotational constant in Cartesian coordinates for NO_3 are presented in Tables 6.1- 6.2. The geometries and L-Matrices used to determine these derivatives were calculated using the CFOUR electronic structure package using a CCSDT basis and were provided via collaboration with Dr. John Stanton.

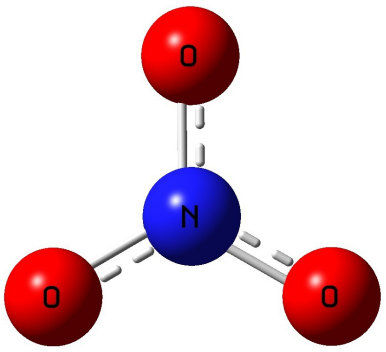

Figure 6.1: Predicted geometry of nitrate radical at the conical intersection with three equivalent Nitrogen-Oxygen bonds.

6.1.2 $\widetilde{A}^2E''$ Vibrationless State h_1'

Three sets of parameters are available for determination of the matrix elements in the first order term of h_1. Two theoretical surfaces are available as well as one experimentally generated surface. The first 'Calculated' surface is generated via electronic structure calculations, while the 'Artificially Generated' surface fit a surface to artificial spectra created via electronic structure means.[15] The experimentally generated surface was generated via fitting the electronic spectra of Figure 6.2.

The two theoretical surfaces are in good agreement to first order contributions to h_1, where as in the case of cyclopentadienyl, the sign represents a choice of phase and could be switched by choice of opposite phase. The potential energy surface generated via fitting the vibrationally resolved spectra estimates a much larger value for h_1'. The experimental magnitude of h_1 isn't as well determined for NO_3 as for C_5H_5, but is bounded above at 0.0025 cm^{-1}. Clearly in this case, the agreement between the first order h_1' and experimental values isn't as excellent as was the case in the cyclopentadienyl radical.

6.1.3 Comparing Theory and Experiment

The lack of agreement between the calculated magnitudes of h_1' upon first inspection might appear to degrade the applicability of the derived methodology to any Jahn-Teller active molecule. However, much stronger Jahn-Teller effects in NO_3 than C_5H_5 allows for a better

understanding of assumptions made in the Taylor expansion derivation.

Higher Order Terms

In calculating h_1', h_1 is approximated as exclusively the first term of a Taylor expansion. As is the case when expressing complex quantities as polynomial expansions, higher accuracy is achieved by including higher order terms of the expansion. In C_5H_5, the weak Jahn-Teller effect in combination with the fact that different symmetry vibrational modes are only linearly or quadratically Jahn-Teller, generates small second order corrections to h_1 as is seen in Tables 5.12- 5.13. In NO_3, a stronger Jahn-Teller effect causes these second order terms, h_1'', to be more significant with respect to first order terms, h_1'. Initial results show h_1'' to be approximately the same magnitude as h_1' for the vibrationless state, indicating higher order corrections than h_1' are required for the best prediction of h_1.

Quadratic Hamiltonian

While higher order corrections to h_1 lead to approximate agreement between the computational parameters generated and experimentally determined h_1 values, the calculated h_1 from an experimental surface remains an outlier. The parameters of Table 6.3 were determined by fitting the experimental spectra of 6.2 to a parameterized quadratic Hamiltonian model. Here, it is assumed that the quadratic model is able to fully capture the details of the potential energy surface. Inspection of Figure 2.2 reveals a much more complex surface than can be simply modeled by quadratic functions. In this way, the experimentally determined parameters are insufficient to describe the complex surface, and thus generate inaccurate eigenfunctions needed to calculate h_1. The insufficiency of the quadratic Hamiltonian has been extensively studied and shown elsewhere[15] To reconcile the experimental and theoretical values, a higher order Hamiltonian is required to fit the electronic spectra and generate more precise vibronic parameters.

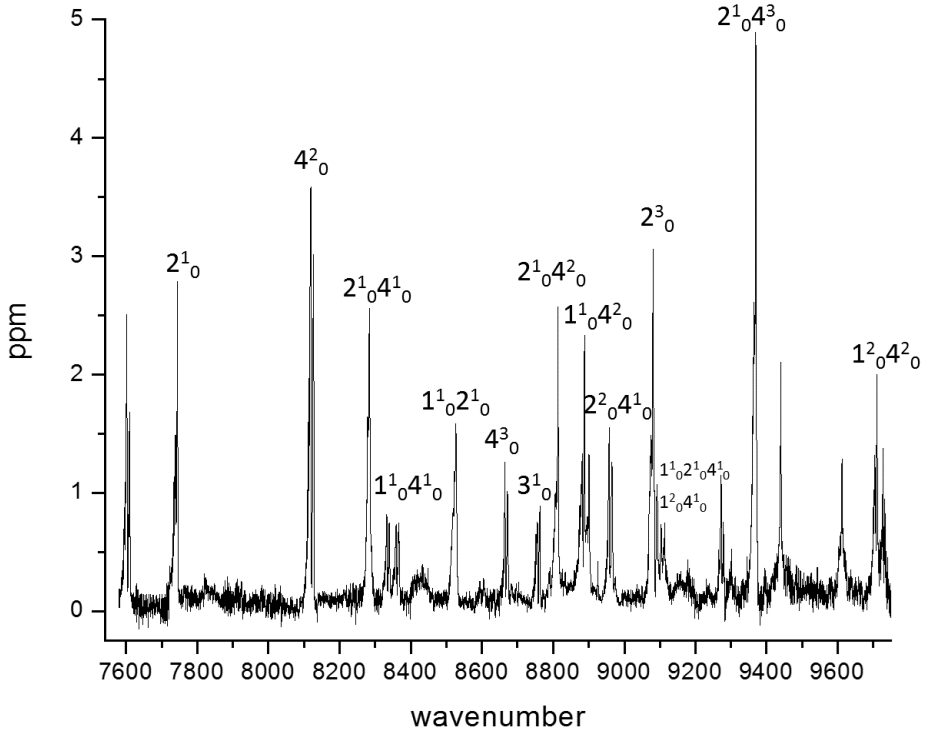

Figure 6.2: Electronic spectra of $\widetilde{A}^2E'' \leftarrow \widetilde{X}^2A_2'$ transition of NO_3 taken by Codd to which parameters of Table 6.3 Experimentally Generated Surface were fit.[13]

Vibrational Mode	$\frac{\partial I_{xx}}{\partial q_i}$	$\frac{\partial I_{xy}}{\partial q_i}$	$\frac{\partial I_{xz}}{\partial q_i}$	$\frac{\partial I_{yx}}{\partial q_i}$	$\frac{\partial I_{yy}}{\partial q_i}$	$\frac{\partial I_{yz}}{\partial q_i}$	$\frac{\partial I_{zx}}{\partial q_i}$	$\frac{\partial I_{zy}}{\partial q_i}$	$\frac{\partial I_{zz}}{\partial q_i}$
q_1	-5.6508541	0	-5.7279668e-05	0	-11.301051	0	-5.7279668e-05	0	-5.6501964
q_2	0	0	0	0	0	0	0	0	0
q_{3a}	1.3150333	0	0	0	0	0	0	0	-1.3150333
q_{3b}	0	0	1.3150334	0	1.5069324e-07	0	1.3150334	0	1.5226454e-07
q_{4a}	-6.5328337	0	0	0	0	0	0	0	6.5328336
q_{4b}	0	0	-6.5328337	0	0	0	-6.5328337	0	0

Table 6.1: First derivatives of inertial tensor for NO_3 calculated using third order finite differentiation with stepsize of 1e-05. Units are amu^{1}bohr^2. The molecule lies in the xy plane.

Vibrational Mode	$\frac{\partial B_{xx}}{\partial q_i}$	$\frac{\partial B_{xy}}{\partial q_i}$	$\frac{\partial B_{xz}}{\partial q_i}$	$\frac{\partial B_{yx}}{\partial q_i}$	$\frac{\partial B_{yy}}{\partial q_i}$	$\frac{\partial B_{yz}}{\partial q_i}$	$\frac{\partial B_{zx}}{\partial q_i}$	$\frac{\partial B_{zy}}{\partial q_i}$	$\frac{\partial B_{zz}}{\partial q_i}$
q_1	0.018191132	0	1.8439372e-07	0	0.0090950368	0	1.8439372e-07	0	0.018189015
q_2	0	0	0	0	0	0	0	0	0
q_{3a}	-0.0042333324	0	0	0	0	0	0	0	0.0042333325
q_{3b}	0	0	-0.0042333329	0	0	0	-0.0042333329	0	0
q_{4a}	0.021030386	0	0	0	0	0	0	0	-0.021030385
q_{4b}	0	0	0.021030386	0	0	0	0.021030386	0	0

Table 6.2: Derivatives of rotational constant of NO_3 calculated utilizing the relations of Equation 3.11 and the derivatives of the inertial tensor from Table 6.1. Units are wavenumber. The molecule lies in the xy plane.

Surface Source	Calculated [1]	Artificially Generated[2]	Experimentally Generated[3]
q_1 Frequency (Totally Symmetric $a_1^{'}$)	1034	1005.89	781.4
q_3 Frequency	1105	1212.69	1433.6
D_3 (unitless)	(-)1.90522	(-)1.782	3.20
K_3 (unitless)	0.265158	0.2794	0.245
q_4 Frequency	636	664.91	528.4
D_4 (unitless)	(-)0.17849	(-)0.2605	0.0
K_4 (unitless)	-0.12421	-0.1282	0.0212
q_1/q_3 Coupling	-123	132.675	0
q_1/q_4 Coupling	-51	57.6295	0
q_3/q_4 Coupling	-52	-22.5206	0
Calculated $h_1^{\prime}$	-0.00100	0.001201	0.00692
Experimentally Determined h_1 Magnitude[4]	< 0.0025		

Table 6.3: [1] Parameters taken from Reference[32] [2] Taken from Reference[15] [3] Taken from Reference[13] [4] Taken from Reference.[31] All values have units of wavenumber unless stated otherwise.

Chapter 7
Conclusion

Generalized methodology for the determination of the Watson term, h_1, has been developed in concert with software infrastructure for the calculation of this parameter via solely *ab initio* electronic structure calculations. The cyclopentadienyl and nitrate radicals have been analyzed in this way, opening the door for high resolution vibrational spectra to have bands assigned by their rotational structure.

Tested against the vibrationless state of the cyclopentadienyl radical, h_1 to both a first and second order approximation, agrees with experimentally determined values. Calculated h_1 values for vibrationally excited states up to and including the C-H stretch region are now available for the identification of vibrational bands via rotational structure. For the nitrate radical, calculated magnitudes of h_1' from parameters available via electronic structure methods and experimental methods give poor agreement both between theoretical and experimental vibronic parameters as well as with h_1 magnitudes via fitting rotational spectra. The calculated and experimental agreement can be improved by including higher order terms of the Taylor expansion.

The methodology to calculate h_1 is a necessary component for calculating entire rovibronic spectra of Jahn-Teller molecules via exclusively *ab initio* methods. Extension of this methodology to calculating other rotational parameters, such as h_2, from vibronic functions allows for greater abilities to understanding the spectra of complex chemical processes and reaction mechanisms that proceed through Jahn-Teller molecules.

Bibliography

[1] J. Chappuis. Ann. d. l'ecole norm. sup. *Norm. Sup.*, 11:159.

[2] E. J. Jones and O. R. Wulf. *J. Chem Phys*, 5:876.

[3] R. P. Wayne, I. Barnes, P. Biggs, J. P. Burrows, C. E. Canosa-Mas, J. Hjorth, G. Le Bras, G. K. Moortgat, D. Perner, G. Poulet, G. Restelli, and H. Sidebottom. The nitrate radical: Physics, chemistry, and the atmosphere. *Atmospheric Environment*, 25:1–203, 1991.

[4] J.P D.; Leaitch W.R.; Li S-M.; Sjostedt S.J.; Wentzell J.J.B.; Liggio J.; Macdonald A.M. Lee, A.K.Y; Abbatt. Substantial secondary organic aerosol formation in a coniferous forest: Observations of both day-and nighttime chemistry. *Atmos. Chem. Phys.*, 16:6721–6733.

[5] Gerald R. Liebling and Harden M. McConnell. Study of molecular orbital degeneracy in c5h5. *The Journal of Chemical Physics*, 42(11):3931–3934, 1965.

[6] Lawrence C. Snyder. Jahnteller distortions in cyclobutadiene, cyclopentadienyl radical, and benzene positive and negative ions. *The Journal of Chemical Physics*, 33(2):619–621, 1960.

[7] Ira Levine. *Quantum Chemistry*. Pearson, 7 edition, 2013.

[8] H. A. Jahn and E. Teller. Stability of polyatomic molecules in degenerate electronic states. i. orbital degeneracy. *Proc. Royal Soc.*, 161, 1937.

[9] Timothy A. Barckholtz and Terry A. Miller. Quantitative insights about molecules exhibiting jahn-teller and related effects. *International Reviews in Physical Chemistry*, 17(4):435–524, 1998.

[10] Vadim L. Stakhursky, Ilias Sioutis, György Tarczay, and Terry A. Miller. Computational investigation of the jahn-teller effect in the ground and excited electronic states of the tropyl radical. part i. theoretical calculation of spectroscopically observable parameters. *J. Chem. Phys.*, 128, 2008.

[11] J. K. G. Watson. Jahn-teller and l-uncoupling effecs on the rotational energy levels of symmetric and spherical top molecules. *J. Mol. Spec.*, 103:125–146, 1984.

[12] Lian Yu, Stephen C. Foster, James M. Williamson, Michael C. Heaven, and Terry A. Miller. Rotationally resolved electronic spectrum of jet-cooled cyclopentadienyl radical. *The Journal of Physical Chemistry*, 92(15):4263–4266, 1988.

[13] Terrance J. Codd. *Spectroscopic Studies of the $\tilde{A}^2E''$ State of NO_3*. PhD thesis, The Ohio State University, 2014.

[14] Lucien Henry and Gilber Amat. Sur les coefficients d'interaction entre la vibration et la rotation dans les molecules polyatomiques. ii. pages 230–256.

[15] Henry Tran. *Analysis of the Jahn-Teller Effect on The Spectrum and Structure of the NO3 Radical*. Undergraduate research thesis.

[16] Henry K. Tran, John F. Stanton, and Terry A. Miller. Quantifying the effects of higher order coupling terms on fits using a second order jahn-teller hamiltonian. *Journal of Molecular Spectroscopy*, 343:102 – 115, 2018. Spectroscopy of Large Amplitude Vibrational Motion, on the Occasion of Jon Hougens 80th Birthday Part II.

[17] C. di Lauro. Matrix elements of the powers of q and p operators for the isotropic two-dimensional oscillator. *Journal of Molecular Spectroscopy*, 41(3):598 – 599, 1972.

[18] B. A. Thrush. Spectrum of the cyclopentadienyl radical. *Nature*, 21 July 1956.

[19] Terry A. Miller M. Heaven, L. DiMauro. Laser induced fluorescence spectra of free-jet cooled organic free radicals. vinoxy, cyclopentadienyl and benzyl. *Chemical Physics Letters*, 95(45), March 1983.

[20] V. A. Korolev and O. M. Nefedov. Direct ir spectroscopic study of the cyclopentadienyl radical. *Russian Chemical Bulletin*, 42(8):1436–1437, Aug 1993.

[21] Brian E. Applegate, Terry A. Miller, and Timothy A. Barckholtz. The jahnteller and related effects in the cyclopentadienyl radical. i. the ab initio calculation of spectroscopically observable parameters. *The Journal of Chemical Physics*, 114(11):4855–4868, 2001.

[22] Brian E. Applegate, Andrew J. Bezant, and Terry A. Miller. The jahnteller and related effects in the cyclopentadienyl radical. ii. vibrational analysis of the 2a2x2e1 electronic transition. *The Journal of Chemical Physics*, 114(11):4869–4882, 2001.

[23] Daniel Leicht, Matin Kaufmann, Gerhard Schwaab, and Martina Havenith. Infrared spectroscopy of the helium solvated cyclopentadienyl radical in the ch stretch region. *The Journal of Chemical Physics*, 145(7):074304, 2016.

[24] John F. Stanton David Nesbitt Ketan Sharma, Terry A. Miller. The rovibronic spectra of the cyclopentadienyl radical. In *72nd International Symposium on Molecular Spectroscopy*.

[25] John F. Stanton. On the vibronic level structure in the NO_3 radical: I. the ground electronic state. *J. Chem. Phys.*, 126:134309, 2007.

[26] J. F. Stanton and M. Okumura. On the vibronic level structure in the NO_3 radical part III. observation of intensity borrowing via ground state mixing. *Phys. Chem. Chem. Phys.*, 11:4742, 2009.

[27] J. F. Stanton. On the vibronic level in the NO_3 radical: II. adiabatic calculation of the infrared spectrum. *Mol. Phys.*, 107:1059, 2009.

[28] Eizi Hirota, Kentarou Kawaguchi, Takashi Ishiwata, and Ikuzo Tanaka. Vibronic interactions in the no_3 radical. *J. Chem. Phys.*, 95(2):771, July 1991.

[29] Christopher S. Simmons, Takatoshi Ichino, and John F. Stanton. The ν_3 fundamental in no_3 has been seen near 1060 cm^{-1}, albeit some time ago. *J. Phys. Chem. Lett.*, 3:1946–1950, 2012.

[30] E. Hirota, T. Ishiwata, K. Kawaguchi, M. Fujitake, N. Ohashi, and I. Tanaka. Near-infrared band of the nitrate radical of NO_3 observed by diode laser spectroscopy. *J. Chem. Phys.*, 107:2829, 1997.

[31] Terry A. Miller. The jahn-teller effect and degeneracy breaking in free radicals: Reconciling theory and experiment. In *34th International Symposium on Free Radicals.*

[32] T. Codd, M.-W. Chen, M. Roudjane, J.F. Stanton, and T.A. Miller. Jet cooled cavity ringdown spectroscopy of the $\widetilde{A}^2E'' \leftarrow \widetilde{X}^2A_2'$ transition of the NO_3 radical. *J. Phys. Chem.*, 142:184305, 2015.